Large-wavelength late Miocene thrusting in the North Alpine foreland: Implications for late orogenic processes

Samuel Mock[1], Christoph von Hagke[2], Fritz Schlunegger[1], István Dunkl[3], Marco Herwegh[1]

[1]Institute of Geological Sciences, University of Bern, Baltzerstrasse 1+3, 3012 Bern, Switzerland
5   [2]Institute of Geology and Palaeontology, RWTH Aachen University Wüllnerstrasse 2, 52056 Aachen, Germany
[3]Geoscience Center, Sedimentology and Environmental Geology, University of Göttingen Goldschmidtstrasse 3, 37077 Göttingen, Germany

Correspondence to: Samuel Mock (samuel.mock@geo.unibe.ch)

Abstract. Additional to classical nappe tectonics, the Oligocene to mid-Miocene post-collisional evolution of the Central
10 European Alps was characterized by vertically directed tectonics, with backthrusting along the Insubric Line and the subsequent uplift of the External Crystalline Massifs (ECMs). Thereafter, the orogen experienced axis-perpendicular growth when deformation propagated into its external parts. For the North Alpine foreland between Lake Geneva and Lake Constance, in the past, this has been kinematically and spatially linked to the uplift and exhumation of the ECMs. Based on apatite (U-Th-Sm)/He thermochronometry, we constrain thrusting in the Subalpine Molasse between 12-4 Ma, thus occurring coeval to
15 main deformation in the Jura fold-and-thrust belt (FTB) and late stage exhumation of the ECMs. However, this pattern of tectonic activity is not restricted to areas which are bordered by ECMs, but is consistent along the northern front of the Alps between Geneva and Salzburg. Therefore, late Miocene foreland deformation is not necessarily a consequence of uplift and exhumation of the ECMs. While the local geometry of the Subalpine Molasse results from lateral variations of the mechanical stratigraphy of the foreland basin sediments, we suggest that the large-wavelength tectonic signal is the response to a shift in
20 tectonic forces possibly caused by deep-seated geodynamic processes. This resulted in a change from dominantly vertical to horizontal tectonics and orogen-perpendicular growth of crustal thickening. We constrain the onset of this major tectonic change to ca. 12 Ma in the North Alpine foreland, resulting in thrusting and folding in the Subalpine Molasse west of Salzburg and in the Jura FTB until at least 4 Ma.

1 Introduction

25 Deep crustal processes and slab dynamics have been considered to strongly influence the evolution of mountain belts (e.g., Davies and von Blanckenburg, 1995; Molnar et al., 1993; Oncken et al., 2006). However, these deep-seated signals may be masked by tectonic forcing at upper crustal levels and by enhanced surface erosion related to climate change (e.g. Champagnac et al., 2007; Chemenda et al., 2000; Ganti et al., 2016; Whipple, 2009; Willett et al., 2006). In near surface crustal domains, it is thus challenging to isolate the exhumation signal related to slab dynamics. In this context, foreland basins offer suitable
30 archives as they potentially bear information that allows to resolve the influence of deep-seated processes on mountain

building. This is the case because these basins not only record signals that are related to surface dynamics such as changes of sediment fluxes and eustacy (e.g. Pippèrr and Reichenbacher, 2017; Sinclair and Allen, 1992). They also preserve information on tectonic processes at the crustal and possibly mantle scales that operate at long timescales and large wavelengths (e.g. DeCelles and Giles, 1996; Garefalakis and Schlunegger, 2018; Leary et al., 2016). The North Alpine foreland basin, or Molasse

5 Basin, is particularly suited to constrain the geodynamic evolution of the collisional Alpine orogen because the history of this sedimentary trough has been well established through numerous magneto- and tectonostratigraphic (e.g. Burkhard and Sommaruga, 1998; Ganss and Schmidt-Thomé, 1953; Homewood et al., 1986; Kempf et al., 1999; Pfiffner, 1986; Schlunegger et al., 1996; Sinclair et al., 1991), seismic (Hinsch, 2013; Mock and Herwegh, 2017; Ortner et al., 2015; Sommaruga et al., 2012), and low-temperature thermochronological analyses (Cederbom et al., 2004, 2011; Gusterhuber et al., 2012; von Hagke

10 et al., 2012, 2014b; Mazurek et al., 2006).

Studies from the forelands of the European Alps have shown that the most external parts of the orogen were incorporated into the orogenic wedge in Miocene times (Becker, 2000; Burkhard, 1990; von Hagke et al., 2012, 2014b; Hinsch, 2013; Ortner et al., 2015; Pfiffner, 1986; Schmid et al., 1996; Schönborn, 1992). In the case of the Swiss Molasse Basin, late Miocene deformation has been kinematically and spatially linked to the uplift and exhumation of the External Crystalline Massifs

15 (ECMs) derived from the subducting European plate, and to main deformation in the Jura fold-and-thrust belt (FTB) situated at the northern margin of the Molasse Basin (Figs. 1 and 2; e.g. Burkhard, 1990; Burkhard and Sommaruga, 1998; von Hagke et al., 2014b; Laubscher, 1992; Mosar, 1999; Pfiffner, 1986; Sommaruga, 1999). The inferred linkages between uplift of the ECMs, imbrication of the proximal Molasse deposits, and main deformation in the Jura FTB are mainly based on a classical scenario of late-stage continent-continent collision, where compressional wedge tectonics and shortening result in a

20 propagation of the orogenic wedge towards the foreland, including imbricate thrusting (Pfiffner, 1986; Rosenberg and Berger, 2009; Schmid et al., 1996). However, foreland propagation of deformation was not continuous as shown by structural, chronostratigraphic, and low-temperature thermochronological data, indicating that the Alpine thrust front advanced rather discontinuously during Miocene times (Beidinger and Decker, 2014; Burkhard and Sommaruga, 1998; von Hagke et al., 2014b; Ortner et al., 2015). In addition, the along strike partitioning of strain between the Jura FTB and the Subalpine Molasse has

25 only incompletely been resolved so far. In the same sense, it has been unclear whether the amount of shortening within the Subalpine Molasse is consistent along strike, particularly with respect to the highly non-cylindrical architecture of the Alpine hinterland (Fig. 2). However, this information is vital for understanding how deformation in the ECMs is potentially linked to foreland FTB tectonics. Accordingly, as a first and major contribution of our paper, we aim at reconstructing the chronology and amount of shortening of the Molasse sequences during the late stage of Alpine orogeny since the mid-Miocene. Hereto,

30 we build upon detailed and well-established work on the chronology, tectonics, and stratigraphy of the proximal foreland (e.g. Burkhard and Sommaruga, 1998; von Hagke et al., 2012, 2014b; Hinsch, 2013; Kempf et al., 1999; Ortner et al., 2015; Pfiffner, 1986; Schlunegger et al., 1997; and many others). We will relate these mechanisms to the history of shortening of the Jura FTB, and to Alpine tectonic events in an effort to identify relationships to possible geodynamic forcing at the larger scale.

Geological mapping of the Subalpine Molasse (e.g. Ganss and Schmidt-Thomé, 1953; Haldemann et al., 1980; Schlunegger et al., 2016; Weidmann et al., 1993; Zaugg et al., 2011) as well as stratigraphic work (e.g. Bachmann and Müller, 1992; Kempf et al., 1999; Lemcke, 1988; Schlunegger et al., 1993, 1997; Schlunegger and Kissling, 2015) has shown that the proximal basin border is characterized by large orogen-parallel lithologic variations where km-thick conglomerate suites with high mechanical

5 strengths alternate with mudstones and sandstones with low at-yield conditions over lateral distances of a few kilometers. As a consequence, the patterns of thrust faults and folds within the Subalpine Molasse change along-strike. In regions where the km-thick conglomerate packages are present, the geometry of the Subalpine Molasse is characterized by km-spaced thrust faults with a relatively large displacement. In areas however, where the foreland mechanical stratigraphy consists mostly of sandstone-mudstone alternations, the structural style is characterized by closely-spaced folds and thrust faults with possibly

10 smaller displacements. We expect that these differences in mechanical stratigraphy leave a distinct imprint on where strain is accommodated during late orogenic shortening. Therefore, as a related second contribution, we aim at exploring how lithological variations within the foreland basin, which were controlled by the paleogeographic conditions, contributed to the spatial distribution of late orogenic strain.

In summary, we present new low-temperature thermochronological data from a key region in the western Subalpine Molasse

15 and compare them with previously published data from farther east (von Hagke et al., 2012, 2014b). We combine this with tectono-sedimentological data along the thrusted Subalpine Molasse between 6.8° E (Lake Geneva) and 12.8° E (near Salzburg) in order to better constrain the timing and spatial pattern of thrusting in the Subalpine Molasse and the associated late-orogenic large-scale change from dominantly vertical to dominantly horizontal tectonics.

2 Geological and tectonic setting

20 ### 2.1 The Central Alps

We focus our study on the Central Alps because the inversion of the proximal basin part by imbricate tectonics during late Miocene times terminates near Salzburg (Fig. 1). This is also the region where the configuration of the lithospheric mantle slabs at depth changes along-strike. Seismo-tomography studies have disclosed that the subducting European slab beneath the Central Alps extends to the east until ca. 12.5° E, i.e. the area of Salzburg, while farther east, a segmentation of the slab

25 structure is observed (Kästle et al., 2019; Lippitsch et al., 2003; Mitterbauer et al., 2011; Zhao et al., 2016; see further details in the discussion section). Classically, the boundary (or transition) between the Central and the Eastern Alps has been located in eastern Switzerland where remnants of the Piemont-Ligurian Ocean separate units deriving from the former European passive margin (Central and Western Alps) from units deriving from the Adriatic Plate north of the Insubric Line (Figs. 1 and 2; Eastern Alps; Schmid et al., 2004). However, we place the boundary between the Central and Eastern Alps farther east

30 where the current slab configuration changes at depth, following hereby a definition recently used by others (Kissling and Schlunegger, 2018; Rosenberg et al., 2018). This is particularly important when the influence of subduction mechanisms on

the surface geology during the past few millions of years is addressed, which is the scope upon discussing the results at the end of this paper. We will therefore focus in this section on the geological and tectonic setting of the Central Alps, but will elaborate on influences of Eastern Alpine tectonic processes in the discussion part of this paper.

The Central Alps are situated almost entirely on top of the subducted Central European lithospheric slab (Figs. 2a and 2b; Schmid et al., 1996, 2017), which steeply dips into the asthenospheric mantle as imaged by teleseismic tomography (Lippitsch et al., 2003). The bivergent orogen is the result of Late Cretaceous to Eocene ocean-continent subduction of the European plate under the Adriatic plate and subsequent post-35 Ma continent-continent collision (e.g. Schmid et al., 1996). The subduction system became clogged when the thick and buoyant European crust started to enter the subduction zone, which resulted in oceanic slab breakoff ca. 32 Myr ago (Davies and von Blanckenburg, 1995). Slab unloading and basal accretion of crustal segments to the upper plate resulted in a period of fast uplift, which was mainly accommodated through backthrusting along the Insubric Line (Hurford, 1986; Schmid et al., 1996). The signal of slab breakoff is also manifested in the rapid build-up of topography and in the subsequent increase of sediment discharge into the Alpine foreland (Schlunegger and Castelltort, 2016; Sinclair, 1997). Recently, the idea of slab breakoff has been challenged and instead the volcanic and tectonic signal has been attributed to slab-steepening and consequently enhanced corner flow (Ji et al., 2019). During the Oligocene, Europe-derived sedimentary units were sheared off from their substratum and emplaced to the north over several tens of kilometers forming the present-day Helvetic cover nappes (Pfiffner, 2011, and references therein). Ongoing orogeny resulted in delamination of lower European crustal segments (Fry et al., 2010), eventually inducing buoyancy-driven subvertical uplift (vertical tectonics) of the thickened crust (Kissling and Schlunegger, 2018) along steeply dipping shear zones and exhumation of the ECMs ca. 20 Myr ago (Fig. 2a; Herwegh et al., 2017, in press). Farther east, between the Aar Massif and the Brenner Fault (a segment, which we here consider as the eastern Central Alps), such Europe-derived crustal blocks are not exposed at the surface. East of the Brenner Fault (Fig. 1), northward indentation of the Dolomite indenter resulted in eastward lateral extrusion of crustal blocks, which started in early Miocene times (Frisch et al., 1998; Handy et al., 2015; Ratschbacher et al., 1991). Associated with this was the exhumation of the Tauern Window and normal faulting along its bounding low-angle normal faults (see Rosenberg et al., 2018).

The late stage in the evolution of the Central Alps is dominated by orogen-perpendicular growth due to the propagation of deformation to its external parts, i.e., to the Molasse Basin and the Jura fold-and-thrust belt (FTB) in the north, and to the Southern Alps in the south (Figs. 1 and 2; Burkhard, 1990; Caputo et al., 2010; Castellarin and Cantelli, 2000; Nussbaum, 2000; Pfiffner, 1986; Schmid et al., 1996; Schönborn, 1992), thereby marking a change from dominantly vertical to horizontal tectonics (Schlunegger and Simpson, 2002). In the Southern Alps, fold-and-thrust belts evolved from late Oligocene times on onwards, but the largest amounts of shortening occurred after ca. 15 Ma (Caputo et al., 2010; Castellarin and Cantelli, 2000; Schmid et al., 1996; Schönborn, 1992).

2.2 The Molasse Basin

The Molasse Basin of the North Alpine foreland, which contains erosional products of the evolving Alps since 32 Ma (Sinclair et al., 1991), is tectonically subdivided into three parts: (i) The Plateau Molasse is the gently folded part of the basin, which evolved into a wedge-top basin during late Miocene main Jura FTB deformation, when it became detached above a main

5   décollement zone within the Triassic evaporites. (ii) To the east, with the Triassic evaporites diminishing and the Jura FTB tapering off, the basin gradually changes into a non-detached configuration, the Foreland Molasse. (iii) At the southern, proximal basin border, the Subalpine Molasse extends continuously as a narrow band of imbricates from south of Geneva to Salzburg, where it disappears below Helvetic and Penninic units before it emerges again in upper Austria. In this contribution we mainly focus on the Subalpine Molasse between Lake Geneva and Salzburg, i.e. the part of the fold-thrust belt that can be

10 considered being associated with the European lithospheric slab of the Central Alps.

The Subalpine Molasse consists of south-dipping imbricated thrust sheets and in large parts of north-dipping backthrusts forming a triangle zone at the transition to the Plateau and Foreland Molasse (Fig. 2; Berge and Veal, 2005; Fuchs, 1976; Müller et al., 1988; Ortner et al., 2015; Schuller et al., 2015; Sommaruga et al., 2012). The Subalpine Molasse started to become incorporated into the orogenic wedge shortly after deposition in Oligocene times (Hinsch, 2013; Kempf et al., 1999;

15 Pfiffner, 1986). After ca. 20 Ma, contemporaneously with the development of the frontal triangle zone, the northern Alpine thrust front remained stationary in the area of the Subalpine Molasse (Burkhard and Sommaruga, 1998; von Hagke et al., 2014b; Ortner et al., 2015). It was not until ca. 12 Ma when parts of the deformation in the western Molasse Basin (i.e. the Molasse west of Lake Constance) propagated along a basal décollement zone within the Triassic evaporites into the thin-skinned Jura FTB (Becker, 2000; Burkhard and Sommaruga, 1998; Laubscher, 1961; Philippe et al., 1996), although already

20 in the late Oligocene some deformation occurred in the area of the today's Jura FTB (Aubert, 1958; Liniger, 1967). Hence, during the late Miocene, the Molasse Basin experienced along-strike changes in tectonic style and locus of deformation. While sediment accumulation in the eastern Molasse Basin (i.e. here the Foreland Molasse between Lake Constance and Salzburg) occurred still in a foredeep setting, the western part evolved at this stage into a wedge-top basin (i.e. Plateau Molasse; Willett and Schlunegger, 2010), as it was detached above the basal décollement zone. Both, the evaporite basal décollement and the

25 thrusts of the Subalpine Molasse are considered to root below and in the ECMs. Accordingly, they were kinematically linked to the late Miocene exhumation of the ECMs (Fig. 2a; e.g. Burkhard, 1990), which was driven at that time by north-directed thrusting (Herwegh et al., 2017, in press), thereby causing a phase of accelerated exhumation at ca. 10 Ma (Glotzbach et al., 2010; Valla et al., 2012; Vernon et al., 2009; Weisenberger et al., 2012). Recently, studies have documented that the Subalpine Molasse was subject to break-back thrusting between ca. 13 Ma and 4 Ma (von Hagke et al., 2012, 2014b; Ortner et al., 2015;

30 Schuller et al., 2015), which was thus coeval to folding and thrusting in the Jura FTB. We note that late Miocene thrusting is not recorded for the Subalpine east of Salzburg (Beidinger and Decker, 2014; Hinsch, 2013; Ortner et al., 2015), i.e. where the deep slab configuration of the Eastern Alps is present.

After 10 Ma, but possibly as late as 5 Ma, the Molasse Basin was uplifted, resulting in basin-scale erosion (Baran et al., 2014; Cederbom et al., 2004, 2011; Genser et al., 2007; Gusterhuber et al., 2012; von Hagke et al., 2012; Mazurek et al., 2006; Schlunegger and Mosar, 2011; Zweigel et al., 1998). Since 5 Ma, compressional thin-skinned tectonics in the wedge-top part of the basin and the Jura FTB are superseded by thick-skinned tectonics (Giamboni et al., 2004; Guellec et al., 1990; Madritsch

5   et al., 2008; Mock and Herwegh, 2017; Mosar, 1999; Philippe et al., 1996; Ustaszewski and Schmid, 2007).

The clastic infill of the Oligocene to Miocene peripheral Molasse Basin consists of the eroded sediments of the evolving Alps, and in the northern parts partly of material shed from the Black Forest and the Bohemian Massif. Accommodation space was formed through subsidence, classically related to flexural bending of the European plate in response to the combined effect of subsurface slab loading and topographic loading of the advancing Alpine thrust wedge during Paleogene and Neogene times

10   (Allen et al., 1991; Burkhard and Sommaruga, 1998; Karner and Watts, 1983; Pfiffner, 1986; Zweigel et al., 1998). For the Central Alps, this view has recently been challenged by Schlunegger and Kissling (2015), who favor a slab rollback mechanism, to explain foreland plate flexuring and accommodation space formation. In this scenario, slab rollback is driven by the interplay between vertically-directed slab loads exerted by the subducted European lithospheric mantle and buoyancy-driven crustal delamination (Kissling and Schlunegger, 2018).

15   In the Swiss part of the basin, the Molasse sediments form two regressive and coarsening upward megasequences (Homewood et al., 1986; Kuhlemann and Kempf, 2002; Schlunegger et al., 2007). The first megasequence describes the transition from Rupelian sedimentation in underfilled conditions to Chattian-Aquitanian sedimentation when the basin was overfilled. The Burdigalian and post-Burdigalian stratigraphic records then chronicle the second megasequence during filled to overfilled conditions (Sinclair and Allen, 1992). West of ca. 11° E, large alluvial megafans developed at the mountain front during the

20   overfilled stage of the basin (Frisch et al., 1998; Kuhlemann and Kempf, 2002; Ortner et al., 2015). In their cores, close to the apex, large conglomerate bodies were deposited, while at the margins, the sedimentation was mainly sand- and mudstone dominated. At the proximal basin border, numerous locally-derived bajada fans discharged sediments into the foreland and thus further contributed to the high along-strike stratigraphic variability at the proximal basin border (Kempf et al., 1999; Schlunegger et al., 1997; Spiegel et al., 2001). Farther east, the Molasse Basin prevailed in an underfilled stage during this

25   time, when sedimentation of sandstones and marls occurred under brackish to shallow marine conditions (Hinsch, 2013; Kuhlemann and Kempf, 2002; Lemcke, 1988; Ortner et al., 2015). Large alluvial fans are missing due to the channelizing effect of the paleo-Inn river, which transported the erosional detritus effectively farther to the east (Frisch et al., 1998; Kuhlemann and Kempf, 2002). For more details on the laterally varying stratigraphy, including Wheeler diagrams, the reader is referred to Kempf et al. (1999), Schlunegger et al. (1997), and Schlunegger and Norton (2013) as well as Hinsch (2013),

30   Kuhlemann and Kempf (2002), Lemcke (1988), and Ortner et al. (2015) for the Molasse Basin west and east of Lake Constance, respectively.

3 Methods

3.1 Sample sites and litho-tectonic architecture

We collected 13 samples across the Subalpine Molasse east and west of Lake Thun for apatite (U-Th-Sm)/He (AHe) dating (Fig. 3). The northernmost samples represent coarse-grained Burdigalian sandstones of the Plateau Molasse. Further to the

5 southwest, we sampled Chattian-Aquitanian and Rupelian sandstones within the Subalpine Molasse. Samples have been collected in the hanging- and footwalls of the individual thrusts (Fig. 3). To control the depositional age of the sediments, samples were taken in the vicinity of sites with known mammal ages and magneto-polarity based chronologies (Schlunegger et al., 1996; Strunck and Matter, 2002) wherever possible.

In the sampling area, mapping shows that the litho-tectonic architecture of the Subalpine Molasse contrasts between both sides

10 of Lake Thun (Fig. 3). On the eastern side, the basin is made up of amalgamated conglomerates and a relatively large spacing between the major thrust faults, while the tectonic style of the Subalpine Molasse to the west of Lake Thun is characterized by more evenly distributed thrust sheets made up of alternated sandstone and mudstone beds. The same pattern can be found along strike where the distribution pattern of conglomerates, sandstones, and mudstones tends to condition the location and the spacing of thrust faults. We thus compiled more details about the geological architecture of the proximal Molasse from

15 published geological maps (Landesgeologie, 2005) and use available tectonic sections (Ortner et al., 2015; Sommaruga et al., 2012) to illustrate the related tectonic style.

3.2 (U-Th-Sm)/He (AHe) thermochronology and thermal modeling

We determined the most recent exhumation history of the Subalpine Molasse through AHe dating. This method is based on the α-decay of ^{238}U, ^{235}U, ^{232}Th and ^{147}Sm isotopes, and the retention of its radiogenic product ^{4}He in the crystal lattice below

20 a certain temperature (e.g., Farley, 2002). Diffusive loss of ^{4}He in the lattice depends on the grain size, shape, chemical composition, distribution of the mother isotopes, radiation damage density, as well as the time-temperature evolution of the crystal (Farley, 2002; Wolf et al., 1996). Consequently, AHe ages can provide estimates when the mineral passed through the diffusion-sensitive temperature interval between ca. 80°C and 40°C (Wolf et al., 1996), which is referred to as the partial retention zone (PRZ). Hence, this technology allows constraining the tectono-thermal history of the studied rocks in the

25 uppermost few kilometers of Earth's crust. Detrital apatite grains deposited in sedimentary basins primarily carry a cooling history of the hinterland at the time of erosion. Subsequent burial due to sedimentation or tectonic loading may reheat the detrital grains to temperatures above the closure temperature, thereby resetting the chronometer. Subsequent exhumation will chronicle the basin's exhumation, whereas grains that have not been reset during the basin's burial history still carry a signal of older cooling events. Consequently, the relation between cooling age and stratigraphic age may provide estimates on the

30 burial as well as the exhumation history (e.g., Reiners and Brandon, 2006).

We used a combination of standard techniques for the separation of apatite minerals, which particularly includes electrodynamic disaggregation, and magnetic and heavy liquid separation. Single crystals were handpicked under a binocular and checked for inclusions and imperfections under an optical microscope with cross-polarized light (more information on the mineral separation techniques and picking criteria are given in Text A1 in the supplementary material). Helium extraction and

5 measurement of parent isotope contents has been conducted at the GÖochron laboratories of University of Göttingen. Raw ages were corrected for α-ejection (Table 1). We measured four to eight single grain ages per sample and calculated average ages using the unweighted arithmetic mean for completely reset samples. We excluded single grain ages for subsequent geological interpretation based on the following criteria (Table 1): (i) high analytical errors (> 10%), (ii) very low U-content (< 10 ppm), (iii) a substantial amount of He on the first re-extract (> 4%), or erroneous old ages stemming most likely from

10 U-Th rich mineral inclusions which produce parentless He. For the latter case, we plotted the He content versus the present-day He production rate in order to detect these ages (for details see Vermeesch, 2008).

We constrained the thermal histories of the sampled sediments (Fig. 4) by modeling of the AHe age data with the HeFTy software (Ketcham, 2005). We gave the algorithm a maximum degree of freedom. Model constraints included the age of sedimentation, the paleo-temperature (Mosbrugger et al., 2005), the present-day annual average temperature, and maximum

15 post-depositional heating rates inferred from maximum sedimentation rates (Schlunegger and Norton, 2015) and a paleo-geothermal gradient of 28°C/km (Schegg and Leu, 1998).

4 Results

4.1 AHe age data

Samples SM-7 and SM-16 from the Plateau Molasse show a wide spread in AHe ages, indicating a partially exhumed fossil

20 PRZ. Hence, they did not experience enough post-depositional heating for a full reset of the thermochronometer (Fig. 3b and Table 1). All other samples show single grain ages reproducing within error. Ages are significantly younger than the corresponding depositional ages and are thus considered to represent completely reset ages (fully exhumed fossil PRZ), hence inferring substantial post-depositional burial and heating.

Average ages for completely reset samples range from 6.0 ± 0.4 Ma to 10.8 ± 0.6 Ma (Fig. 3b and Table 1). All samples from

25 the Subalpine Molasse show post-depositional burial and heating to > 60°C (Fig. 4). Sample SM-7 from the Plateau Molasse did not experience enough post-depositional heating to fully reset the thermochronometer (Fig. 4). Thermal modeling supports the young exhumation of the Subalpine Molasse between 12 Ma and 5 Ma (Fig. 4). The thermal histories of SM-7 and SM-13 indicate an exhumation signal of the Plateau Molasse at ca. 10 Ma.

Samples SM-8, SM-11 and SM-15 were collected from the same tectonic sliver (Figs. 3a and 5), and corresponding average

30 ages of 6.0 ± 0.4 Ma, 6.6 ± 0.4 Ma and 6.1 ± 0.4 Ma reproduce well within error. A jump of average ages occurs to the adjacent

tectonic slivers and the Plateau Molasse in the north, where samples SM-12, SM-13, and SM-14 yield average ages of 9.2 ± 1 Ma, 8.9 ± 0.7 Ma, and 10.8 ± 0.6 Ma, respectively, thus also reproducing within error. This pattern is also reproduced by the modeled thermal histories, where a jump in exhumation ages across tectonic boundaries is recognized (Fig. 4). In the western area, the average ages do not show such a close correlation with the tectonic position (Figs. 3a and 5). However, the thermal

5   models for samples SM-5 and SM-6 indicate younger cooling than for samples SM-4 and SM-7 (Fig. 4), thus suggesting a tectonic control on exhumation.

4.2 Late Miocene shortening estimates

Based on published restored cross-sections (Burkhard and Sommaruga, 1998; von Hagke et al., 2014b; Ortner et al., 2015), balanced maps (Philippe et al., 1996), thermochronological age data (von Hagke et al., 2012, 2014b), and own cross-section

10 restorations, we estimated the amount of late Miocene horizontal shortening of the Subalpine Molasse and the Jura FTB from Lake Geneva to Salzburg (Fig. 6b). Post-12 Ma horizontal shortening in the Jura FTB decreases from a maximum of ca. 32 km in the west to 0 km at the eastern tip (Philippe et al., 1996). Contrariwise, minimum horizontal shortening in the Subalpine Molasse increases from ca. 10 km in the west (Lake Geneva) to ca. 20 km farther east (Lake Constance), before decreasing again to below 1 km in the area near Salzburg (Beidinger and Decker, 2014; Burkhard and Sommaruga, 1998; von Hagke et

15 al., 2012, 2014b; Hinsch, 2013; Ortner et al., 2015). These values do not account for shortening taken up by the frontal triangle zone between ca. 20 Ma and 12 Ma (von Hagke et al., 2014b; Kempf et al., 1999; Ortner et al., 2015). Despite the uncertainty in the shortening estimates within the Subalpine Molasse (Burkhard and Sommaruga, 1998; von Hagke and Malz, 2018; Ortner et al., 2015), we observe that late Miocene cumulative shortening of the Subalpine Molasse and the Jura FTB decreases constantly from the west to the east from >30 km near Geneva to 20 km near Lake Constance, before finally decreasing to <1

20 km near Salzburg (12.8° E; Fig. 6b). It is thus noteworthy that late Miocene shortening in the foreland does not correlate with the peaks of high-uplift domains of the ECMs in the hinterland (Fig. 6c).

5 Discussion

5.1 Downscaling: Local-scale stratigraphic architecture conditioning the pattern of strain release

In the sampling area, mapping discloses along-strike differences in the litho-tectonic architecture of the Subalpine Molasse

25 (Fig. 3). The sediments are thrusted northwestward along SW-NE striking thrusts. East of the Aare valley, a back thrust emerges to the surface and forms a frontal triangle zone (Figs. 3 and 5), a structure which is also known from parts of the Subalpine Molasse farther east (Fig. 7; e.g. Berge and Veal 2005; Müller et al. 1988; Schuller et al. 2015; Sommaruga et al. 2012; Stäuble and Pfiffner 1991, Ortner et al. 2015). The Aare valley, running across the study area, is characterized by a low relief and is filled by >100 m-thick Quaternary deposits (Fig. 5; Dürst Stucki et al., 2010). Accordingly, the structural

30 configuration of this part of the study area is only poorly resolved. However, the structures of the Subalpine Molasse change

abruptly across the Aare valley (Figs. 3 and 5), as has been described by many authors (Beck, 1945; Blau, 1966; Haus, 1937; Pfiffner, 2011; Rutsch, 1947; Vollmayr, 1992). Based on this observation and under the consideration of available interpreted reflection seismic lines, the presence of a possible syn-thrusting strike-slip fault zone running along the valley axis has been proposed (Mock and Herwegh, 2017; Pfiffner, 2011; Vollmayr, 1992). The presence of such a fault is, however, speculative

5 due to the low resolution of the seismic data. An alternative explanation for the sudden along-strike change in the tectonic architecture has first been proposed by Rutsch (1947). He reported that the change from a mainly conglomeratic (east) to a sand- and mudstone dominated (west) lithofacies coincides with an increase in the folding intensity along the frontmost anticline (Falkenfluh anticline; Fig. 3a). Indeed, while conglomerates are the dominant lithofacies in the eastern part of the study area, they are vastly absent west of the Aare valley, where mainly alternating sequences of sandstones and mudstones

10 are outcropping (Figs. 3 and 7; Landesgeologie, 2005). The distribution of mechanically different lithologies seems to control the pattern of strain release (i.e. thrusting pattern). While east of the Aare valley, the mechanically stronger thick conglomeratic sequences deform en-bloc and thrusts are concentrated in narrow bands following mechanically weak zones of sand- and mudstones, strain is released much more distributed along more closely spaced thrusts in the western part of the study area. The pronounced mechanical contrast between conglomerates and sand-/mudstones leads to en-bloc thrusting of the large

15 tectonic slice made up of amalgamated conglomerates east of the Aare valley, and it is also manifested in well-defined and constant AHe ages of ca. 6 Ma (Figs. 3 and 5). AHe ages west of the Aare valley, however, chronicle a more evenly distributed deformation and exhumation pattern, which is most likely conditioned and thus controlled by the low mechanical contrast of the involved lithologies.

The observation that along-strike variations in the stratigraphic architecture lead to complex patterns of strain release is not

20 unique to our sample area, but can be made also at the Mont Pèlerin, the Rigi, or the Hörnli in western, central, and eastern Switzerland, respectively (Fig. 7). In particular, the lithological control on the strain release and exhumation pattern is well observed in the Rigi area (profile 3 in Fig. 7; Sommaruga et al., 2012). The thick conglomerate sequence of the Rigi thrust sheet was (re-)activated en-bloc at ca. 5 Ma, while the adjacent sand- and mudstone dominated part to the north experienced a period of thrusting at ca. 9 Ma along evenly spaced faults (von Hagke et al., 2012). Similar dependencies between the style of

25 deformation and lateral changes in lithology have also been described for the Subalpine Molasse in Bavaria and western Austria (for detailed information see Ortner et al., 2015), as well as for the basal detachments of the Subalpine Molasse and the Jura FTB (von Hagke et al., 2014a). While large alluvial fans deposited thick conglomerate-sandstone sequences in western Bavaria, brackish to shallow marine conditions prevailed farther east where marls and sandstones were deposited (Frisch et al., 1998; Kuhlemann and Kempf, 2002). This lateral change of the Molasse's mechanical stratigraphy has been described to

30 have a direct influence on the deformation style of the Subalpine Molasse (Ortner et al., 2015). While stacks of tectonic horse structures and a pronounced triangle zone developed in western Bavaria, the deformation style changes to buckle folding farther east, which decreases in amplitude and the triangle zone disappears (a detailed description is provided in Ortner et al., 2015).

5.2 Upscaling: Implications for late orogenic processes

5.2.1 The link to exhumation of the External Crystalline Massifs

Classically, thrusting in the Jura FTB and the Subalpine Molasse between Lake Geneva and Lake Constance has been kinematically and spatio-temporally related to the uplift and exhumation of the ECMs, and to the propagation of the deformation front towards the foreland (Burkhard, 1990; Burkhard and Sommaruga, 1998; Pfiffner et al., 1997). However, it has also been reported that the proximal foreland basin east of the easternmost ECM, the Aar Massif, has been subject to post-12 Ma thrusting and horizontal shortening (Figs. 6a and 6b; Ortner et al., 2015). Our AHe age data from the Subalpine Molasse (Figs. 3, 4, and 5) fit with AHe ages farther east (von Hagke et al., 2012, 2014b) and chronicle a period of thrusting and exhumation of the Subalpine Molasse between 12 Ma and 4 Ma (Fig. 6a). This occurred coeval with the main deformation phase in the Jura FTB, which lasted from ca. 12-4 Ma (e.g. Becker, 2000). Similar ages constrained from geological and seismic interpretation, and observations of growth strata in the youngest preserved sediments have been reported for the Subalpine Molasse between Lake Constance and Salzburg (Fig. 6a; Ortner et al., 2015). Based on stratigraphic data, Haus (1935) inferred already in 1935 that the Subalpine Molasse of Central Switzerland was subject to major thrusting in late Miocene times. Since the youngest AHe ages are associated with internal tectonic slices of the Subalpine Molasse (Figs. 3, 4, and 5), we can infer the occurrence of break-back thrusting, a characteristic feature, which has been confirmed so far along the Subalpine Molasse between Bern and Salzburg based on thermochronological data and cross section restorations (von Hagke et al., 2012, 2014b; Ortner et al., 2015; Schuller et al., 2015), but has been locally argued for as early as the 1930s (Haus, 1935, 1937). The break-back thrusts are supposedly younger than the development of the frontal triangle zone, which formed the active northern deformation front from ca. 20-12 Ma (von Hagke et al., 2014b; Ortner et al., 2015). Furthermore, our AHe ages from the Plateau Molasse record a partially exhumed PRZ (Figs. 3, 4, and 5) and thus corroborate the occurrence of substantial exhumation of the flat-lying Plateau and Foreland Molasse (Cederbom et al., 2011; Genser et al., 2007; Gusterhuber et al., 2012; von Hagke et al., 2012; Zweigel et al., 1998), indicating a large wavelength exhumation signal across the entire basin. Because the tectonically driven exhumation signal between 12 Ma and 4 Ma is not unique to the forelands of the ECMs and late Miocene shortening estimates in the North Alpine foreland do not correlate spatially with the high-uplift domains of the ECMs (Fig. 6), we suggest that although kinematically linked, the late Miocene foreland deformation is not a consequence of uplift and exhumation of the ECMs.

5.2.2 Possible link to geodynamic processes beneath the core of the Central Alps

During mid- to late Miocene times, the Central Alps underwent a major change from dominantly vertical to horizontal tectonics. This is also witnessed by the supersession of the vertical extrusion of the ECMs by north-directed thrusting along shallow SE-dipping shear zones (Fig. 8c; Herwegh et al., 2017, in press). In the western North Alpine foreland, large-scale strain partitioning occurred when deformation propagated 50-90 km to the north into the Jura FTB (Becker, 2000) while at the same time the Subalpine Molasse experienced break-back thrusting and thrust reactivation along the entire segment of the Alps

between Lake Geneva and Salzburg (Figs. 6a and 8c). The occurrence of late Miocene thrusting has also been reported for the foreland of the Western Alps (Schwartz et al., 2017). In the Southern Alps, deformation propagated ca. 50 km southward between ca. 15 Ma and 7 Ma (Schmid et al., 1996; Schönborn, 1992).

This rapid change from pre-12 Ma vertical tectonics in the core of the Alps (Herwegh et al., 2017; Hurford, 1986; Schmid et al., 1996), with the triangle zone in the Subalpine Molasse acting as a stationary deformation front from ca. 20-12 Ma (von Hagke et al., 2014b; Ortner et al., 2015), to post-12 Ma orogen-scale horizontal tectonics, accompanied by orogen-perpendicular growth of the Alps, cannot be explained by a classical model of continent-continent collision and continuous foreland propagation of the orogenic wedge. In the following, we discuss the observed exhumation pattern along the Subalpine Molasse (Fig. 6a) in the context of the post-35 Ma tectonic evolution of the Central Alpine orogeny as proposed by Kissling and Schlunegger (2018) and Schlunegger and Kissling (2015) and argue for a deep-driver to control the transition from dominantly vertical to horizontal tectonics, associated with widespread tectonic activity in the foreland and a period of orogenic widening.

During the Alpine orogeny, convergence rates between the Adriatic and European continental plates decreased when the positively buoyant European continental crust started to enter the subduction zone ca. 35 My ago (Fig. 8b; Handy et al., 2010; Schmid et al., 1996) and when delamination and wedging of European continental crust was initiated (Schmid et al., 1996). Large slab pull forces exerted by the negatively buoyant oceanic lithospheric slab induced extensional forces within the subducting plate, which led to necking and eventually to slab breakoff (Davies and von Blanckenburg, 1995). Subsequent slab unloading caused strong uplift and backthrusting along the Insubric Line (Berger et al., 2011; Hurford, 1986; Schmid et al., 1996). According to Kissling (2008) and Kissling and Schlunegger (2018), the delaminated and thus dense European mantle slab, which was still attached to the foreland plate, continued to roll back, with the consequence of slab steepening and northward migration of the locus of crustal delamination. This forced new crustal material to enter the subduction system and to become stacked to the Alpine edifice as evidenced by the emplacement of the Helvetic nappes (Fig. 8c), or was accreted to the crustal root through the basal accretion of mid-crustal material (Fry et al., 2010). Ongoing slab roll back and an associated increase in lower plate flexure resulted in a northward propagation of the northern margin of the Central Alps' Molasse Basin until ca. 20 Ma (Fig. 8a).

Thereafter, plate convergence rates seemed to decrease noticeably (Fig. 8b; Handy et al., 2010; Schmid et al., 1996). At this stage, pro-wedge widening of the Molasse Basin came to a relative halt. In the Central Alps, the proximal part of the basin kept subsiding by additional 2-3 km (Fig. 8a; Burkhard and Sommaruga, 1998; Schlunegger and Kissling, 2015), while the distal realm became subject to erosion (Kuhlemann and Kempf, 2002). This phase was also associated with the period of vertical tectonics of the ECMs, i.e. their rise along steeply dipping shear zones between ca. 20 Ma and 12 Ma (Herwegh et al., 2017; Wehrens et al., 2017), while the northern deformation front remained stationary in the Subalpine Molasse (Fig. 8c; Burkhard and Sommaruga, 1998; von Hagke et al., 2014b; Ortner et al., 2015). East of Munich, however, the Molasse Basin

experienced, at this time, a period of uniform subsidence and even a short-lived phase of uplift (ca. 17-16 Ma) as evidenced by horizontal to 5° westward tilting strata of post-20 My old Molasse sediments (Gusterhuber et al., 2012; Zweigel et al., 1998). This was attributed to a decrease in surface loads in the orogen in response to lateral extrusion (i.e. escape tectonics) and a corresponding lowering of the Eastern Alps' topography (Gusterhuber et al., 2012; Rosenberg et al., 2018). Alternatively,

5   Handy et al. (2015) explained this signal as a result of deep crustal unloading due to a proposed slab tear and a corresponding subduction polarity reversal beneath the Eastern Alps. These observations imply that important along-strike changes and a large-scale geodynamic (Kissling et al., 2006; Lippitsch et al., 2003; Mitterbauer et al., 2011) and tectonic (e.g. Handy et al., 2015; Ratschbacher et al., 1991; Rosenberg et al., 2018) decoupling between the Central and the Eastern Alps and their Molasse Basins have been established by the end of mid-Miocene times.

10   This is also mirrored by the along-strike changes in the late Miocene cumulative shortening in the North Alpine foreland, which decreases from >30 km near Lake Geneva, to ca. 20 km near Lake Constance, and finally to <1 km near Salzburg (Fig. 6). East of Salzburg at the front of the Eastern Alps, zero shortening is recorded in the proximal Molasse. This pattern has been attributed to an increasing transfer of shortening towards the internal parts of the orogen (i.e. the Tauern Window) and to the out-of-section removal of crust through lateral extrusion in the Eastern Alps (Ortner et al., 2006, 2015). While such upper

15   crustal processes may certainly mask the signal of late Miocene foreland deformation, the latter may also reflect the response to the change of a geodynamic driving force operating at a larger scale, situated at deeper crustal levels, and encompassing the entire Central Alps until as far east as 12.8° E (near Salzburg; Fig. 9). The attached European lithospheric slab beneath the Central Alps presents here a possible candidate for driving the observed large wavelength signal of late Miocene foreland deformation (Fig. 9). This hypothesis is based on the following main observations: (i) The along-strike extent of late Miocene

20   thrusting in the foreland correlates spatially remarkably well with the extent of the Central Alpine European slab imaged by seismic tomography (Fig. 9). (ii) The large wavelength of the tectonic signal, which at least in the Subalpine Molasse between Lake Thun and Lake Constance seems to occur in the form of individual tectonic pulses, likely excludes more local upper crustal phenomena as possible drivers and points towards bigger players such as plate tectonics or slab dynamics. (iii) The proposed segmentation of the deep structure of the Central and Eastern Alps (i.e. slab detachment and subduction polarity

25   reversal; Handy et al., 2015; Kästle et al., 2019; Kissling et al., 2006; Lippitsch et al., 2003; Mitterbauer et al., 2011; Schmid et al., 2004), which is expected to have induced a geodynamic and tectonic reorganization along the Alpine chain by the end of mid-Miocene times could explain the subsequent late Miocene tectonism restricted to the foreland of the Central Alps until ca. Salzburg and thus decoupled from the Eastern Alps. The corresponding change in the macro-tectonic regime of the Central Alps from dominantly vertical to large-scale horizontal tectonics may reflect decreasing rates of European slab rollback and a

30   late phase of post-collisional indentation of Adria as recently proposed by Herwegh et al. (2017) and Kissling and Schlunegger (2018).

5.2.3 The exceptional position of the Bavarian Subalpine Molasse

The configuration of the lithospheric mantle slabs is inherently different beneath the Central and the Eastern Alps (Kissling et al., 2006; Kissling and Schlunegger, 2018; Lippitsch et al., 2003; Mitterbauer et al., 2011; Zhao et al., 2016). At the lithospheric scale, a polarity reversal between the European slab and the Adriatic slab has been conjectured beneath the western Tauern Window (Lippitsch et al., 2003). However, this model is currently debated as new geophysical data indicate that at depth the

5   southward dipping European slab extends from the Central Alps until east of the Giudicarie and Brenner Faults (Kästle et al., 2019) and possibly as far east as 12.5° E, i.e. the central Tauern Window (Figs. 1 and 9; Qorbani et al., 2015). Although the tomographic data have been interpreted in different ways regarding the slab geometries at depth (Kästle et al., 2019; Lippitsch et al., 2003; Mitterbauer et al., 2011; Zhao et al., 2016), most of them concur on the observation that between the deep velocity anomalies of the Central and the Eastern Alps a major discontinuity is present east of the Giudicarie and Brenner Faults (see

10 also Handy et al., 2015). This correlates with the eastward termination of the Miocene Subalpine Molasse near Salzburg (Fig. 9). Hence, the geophysical data place the link between the deep structure and deformation of the Subalpine Molasse between Lake Constance and Salzburg in a Central Alpine rather than an Eastern Alpine context.

While at the mantle scale, a segmentation of the slab structure is observed at ca. 12.5° E (Fig. 9), an along-strike segmentation at crustal levels occurs further west (at the Brenner Fault). East of the Brenner Fault (Figs. 1 and 9), the post-collisional

15 evolution of the Eastern Alps is characterized by the northward indentation of the Dolomite indenter and the related eastward lateral extrusion of crustal blocks (Ratschbacher et al., 1991). At the larger scale, this was possibly facilitated by slab retreat beneath the Carpathians and the associated rifting in the Pannonian Basin (Peresson and Decker, 1997). The main phase of lateral extrusion occurred in early and mid-Miocene times (Frisch et al., 1998; Ratschbacher et al., 1991), possibly extending into the late Miocene (Ortner et al., 2015). These processes were additionally associated with the collisional exhumation of the

20 Tauern Window and normal faulting along its bounding low-angle normal faults (see Rosenberg et al., 2018). In this respect, the Bavarian Subalpine Molasse is particularly interesting, since it extends over this transition area (Fig. 9). In this transient position, the tectonics of this segment of the Subalpine Molasse between Lake Constance and Salzburg was probably affected by the deep-seated dynamics of the Central Alpine European slab, while at the same time tectonic processes related to slab dynamics were possibly also masked by upper crustal processes of Eastern Alpine tectonics (e.g. lateral extrusion).

25 For resolving the influence of deep-seated processes on the tectonics of the Subalpine Molasse and the foreland basin in general, the present-day slab geometries underneath the entire Alps must be resolved at higher resolution. Furthermore, the time-evolution of the slabs must be constrained with a focus on if, when, and how a potential subduction polarity reversal occurred in the Eastern Alps. These studies should be supported by source-to-sink analyses linking the stratigraphy of the foreland to hinterland processes. New thermochronological data from the Bavarian Subalpine and Foreland (i.e. undeformed)

30 Molasse will be essential. Furthermore, we expect that ongoing seismo-tomographic investigations will disclose further details to constrain the deep-seated driving mechanisms (Hetényi et al., 2018).

6 Conclusions

In this paper, we presented new low-temperature thermochronological age data from the Subalpine Molasse of the Central European Alps. By comparing our results to published age and stratigraphic data along-strike the Alps from Lake Geneva to Salzburg we conclude that:

- (U-Th-Sm)/He ages along the Subalpine Molasse of the Central Alps are consistently between 12-4 Ma and can be assigned to at least two tectonic pulses at ca. 10 and 6 Ma.
- The pattern of strain release is strongly conditioned by the local-scale mechanical stratigraphy, since the locus of deformation depends on the distribution of mechanically weak (sand- and mudstones) and strong (conglomerates) lithologies.
10
- Despite the along-strike highly non-cylindrical hinterland exhumation history and architecture, the late Miocene tectonic signal recorded in the Subalpine Molasse is remarkably constant along-strike the Alps, from Lake Geneva to Salzburg.

Hence, we observe that the deformation style during late Miocene thrusting of the Subalpine Molasse is masked by local variations in the stratigraphic architecture. However, the overall tectonic signal, though decreasing in intensity from the west
15 to the east, is consistent in terms of timing and kinematics along-strike the part of the Alps which correlates with the lateral (i.e. along-strike) extent of the Central Alpine lithospheric mantle slab at depth. Large-wavelength late Miocene thrusting may thus be interpreted as an upper crustal signal resulting from changes of this lithospheric driving force. The latter possibly leads to a prominent change in the macro-tectonic regime in this sector of the Alpine orogen at ca. 12 Ma, from dominantly vertical to horizontal tectonics.

20 In summary, although we lack the required data to precisely determine the geodynamic processes responsible for the late phase of shortening in the Molasse, we are able to constrain the timing of this event to 12-4 Ma. In addition, this work shows that low-temperature thermochronological data yield an improved understanding of the chronology of orogenic processes where the late orogenic stage of a mountain belt may be characterized by a complex pattern of strain release conditioned by site-specific stratigraphic and thus lithological conditions at the local scale, and by a change from vertical to horizontal tectonics
25 at the larger scale including the entire Central Alps.

Appendix A: Apatite separation and picking

To release the apatite crystals from the rock samples, we used the electrodynamic disaggregation technique (selFrag). This method exposes the rock specimen to a high voltage pulse and fractures it along its grain boundaries. As opposed to separation using a jaw crusher, this method is less time consuming and the rock is disintegrated along the grain boundaries (Giese et al.,
30 2010). This ensures individual grains are less prone to damaging during processing.

To prepare the samples for electrodynamic disaggregation, they had to be crushed into fist-sized pieces by hand using a hammer. This was necessary due to the limiting dimensions of the processing vessel of the selFrag. For releasing the individual grains, we applied a frequency of 3 Hz and electric potentials of 130-150 kV, depending on the hardness of the rock. For every sample, the electrode distance was incrementally reduced in 5 mm steps from a maximum of 40 mm to a minimum of 15 mm.

5 Per step, a minimum of 20 pulses was applied to ensure full release of the individual grains. It has been shown that the influence of diffusive loss of ^{4}He due to the plasma channel hitting the apatite crystal is negligible, and (U-Th-Sm)/He (AHe) ages from samples separated with electrodynamic disaggregation are indistinguishable from AHe ages measured on apatites released with mechanical techniques (Giese et al., 2010).

Apatite crystals were concentrated using standard rock separation techniques. First, the grain size fraction of 64-250 μm, which

10 is suitable for AHe dating, was separated using disposable sieving meshes. To remove magnetic minerals from the sieved sample fraction, we used a Frantz magnetic separator at 0.5 A and 1.2 A. To concentrate apatite from the remaining grains, we used lithium-based tungstate (ρ = 2.81 g cm^{-3}) as heavy liquid for density separation of the heavy minerals. On average, we had to process ca. 100 g of sample material to acquire enough heavy minerals. The heavy mineral fraction has been thoroughly rinsed with deionized water and then dried at 30°C.

15 Apatites have been hand-picked under a binocular and checked for inclusions and imperfections under an optical microscope with cross-polarized light. Wherever possible, we selected euhedral, intact, and inclusion free grains with a minimum width of 60 μm. However, as the grains are detrital, partly grains with rough surfaces or tiny fluid inclusions had to be picked. This may result in larger error bars or even grain ages that do not yield a geologically meaningful age. These ages were excluded (see section 3.2 and Table 1).

20 **Data availability**

The research data is enclosed in this paper and can be freely accessed.

Author contribution

SM designed the study with support from MH, FS, and CvH. FS and MH assisted SM during sampling in the field. SM carried out mineral separation and picked the apatite crystals. ID carried out the helium extraction and the ICP-MS measurements at

25 University of Göttingen. CvH and ID assisted in analyzing and interpreting the apatite (U-Th-Sm)/He ages. SM prepared the manuscript, with contributions from all co-authors.

Competing interests

The authors declare that they have no conflict of interest.

Acknowledgements

We thank Judith Dunkl (Göttingen) for assisting in the selection of apatite crystals, Pierre Valla (Bern) for discussions on the AHe ages and the thermal models, and Edi Kissling (Zurich) for his insights on lithospheric scale processes. The manuscript has greatly benefited by detailed and constructive comments Hugo Ortner (Innsbruck) and Nicola Levi (Vienna). Additional
5 information of the data can be found in the supplementary material. The study was funded by the Swiss Geological Survey of the Federal Office of Topography (swisstopo) as part of the GeoMol CH project. We acknowledge the use of the Move Software Suite (used for Fig. 5) granted by Midland Valley's Academic Software Initiative.

References

Allen, P. A., Crampton, S. L. and Sinclair, H. D.: The inception and early evolution of the North Alpine Foreland Basin,
10 Switzerland, Basin Res., 3(3), 143–163, doi:10.1111/j.1365-2117.1991.tb00124.x, 1991.

Aubert, D.: Sur l'existence d'une ride de plissement oligocène dans le Jura vaudois, Bull. la Société Neuchâteloise des Sci. Nat., 81, 47–54, 1958.

Bachmann, G. H. and Müller, M.: Sedimentary and structural evolution of the German Molasse Basin, Eclogae Geol. Helv., 85(3), 519–530, doi:10.5169/seals-167019, 1992.

15 Baran, R., Friedrich, A. M. and Schlunegger, F.: The late Miocene to Holocene erosion pattern of the Alpine foreland basin reflects Eurasian slab unloading beneath the western Alps rather than global climate change, Lithosphere, 6(2), 124–131, doi:10.1130/L307.1, 2014.

Beck, P.: Über den Mechanismus der subalpinen Molassetektonik, Eclogae Geol. Helv., 38(2), 353–368, 1945.

Becker, A.: The Jura Mountains — an active foreland fold-and-thrust belt?, Tectonophysics, 321(4), 381–406,
20 doi:10.1016/S0040-1951(00)00089-5, 2000.

Beidinger, A. and Decker, K.: Quantifying Early Miocene in-sequence and out-of-sequence thrusting at the Alpine-Carpathian junction, Tectonics, 33(3), 222–252, doi:10.1002/2012TC003250, 2014.

Berge, T. B. and Veal, S. L.: Structure of the Alpine foreland, Tectonics, 24(5), TC5011, doi:10.1029/2003TC001588, 2005.

Berger, A., Schmid, S. M., Engi, M., Bousquet, R. and Wiederkehr, M.: Mechanisms of mass and heat transport during
25 Barrovian metamorphism: A discussion based on field evidence from the Central Alps (Switzerland/northern Italy), Tectonics, 30(1), TC1007, doi:10.1029/2009TC002622, 2011.

Blau, R. V.: Molasse und Flysch im östlichen Gurnigelgebiet (Kt. Bern), Beiträge zur Geol. Karte der Schweiz, NF 125, 151 pp., 1966.

Burkhard, M.: Aspects of the large-scale Miocene deformation in the most external part of the Swiss Alps (Subalpine Molasse to Jura fold belt), Eclogae Geol. Helv., 83(3), 559–583, 1990.

Burkhard, M. and Sommaruga, A.: Evolution of the western Swiss Molasse basin: structural relations with the Alps and the Jura belt, Geol. Soc. London, Spec. Publ., 134(1), 279–298, doi:10.1144/GSL.SP.1998.134.01.13, 1998.

5 Buxtorf, A.: Prognosen und Befunde beim Hauensteinbasis- und Grenchenbergtunnel und die Bedeutung der letzteren für die Geologie des Juragebirges, Verhandlungen der Naturforschenden Gesesellschaft Basel, 27, 184–254, 1916.

Caputo, R., Poli, M. E. and Zanferrari, A.: Neogene–Quaternary tectonic stratigraphy of the eastern Southern Alps, NE Italy, J. Struct. Geol., 32(7), 1009–1027, doi:10.1016/j.jsg.2010.06.004, 2010.

Castellarin, A. and Cantelli, L.: Neo-Alpine evolution of the Southern Eastern Alps, J. Geodyn., 30(1–2), 251–274,
10 doi:10.1016/S0264-3707(99)00036-8, 2000.

Cederbom, C. E., Sinclair, H. D., Schlunegger, F. and Rahn, M. K.: Climate-induced rebound and exhumation of the European Alps, Geology, 32(8), 709, doi:10.1130/g20491.1, 2004.

Cederbom, C. E., van der Beek, P., Schlunegger, F., Sinclair, H. D. and Oncken, O.: Rapid extensive erosion of the North Alpine foreland basin at 5-4 Ma, Basin Res., 23(5), 528–550, doi:10.1111/j.1365-2117.2011.00501.x, 2011.

15 Champagnac, J.-D., Molnar, P., Anderson, R. S., Sue, C. and Delacou, B.: Quaternary erosion-induced isostatic rebound in the western Alps, Geology, 35(3), 195, doi:10.1130/G23053A.1, 2007.

Chemenda, A. I., Burg, J. P. and Mattauer, M.: Evolutionary model of the Himalaya-Tibet system: Geopoem based on new modelling, geological and geophysical data, Earth Planet. Sci. Lett., 174(3–4), 397–409, doi:10.1016/S0012-821X(99)00277-0, 2000.

20 Davies, J. H. and von Blanckenburg, F.: Slab breakoff: A model of lithosphere detachment and its test in the magmatism and deformation of collisional orogens, Earth Planet. Sci. Lett., 129(1–4), 85–102, doi:10.1016/0012-821X(94)00237-S, 1995.

DeCelles, P. G. and Giles, K. A.: Foreland basin systems, Basin Res., 8(2), 105–123, doi:10.1046/j.1365-2117.1996.01491.x, 1996.

Dürst Stucki, M., Reber, R. and Schlunegger, F.: Subglacial tunnel valleys in the Alpine foreland: an example from Bern,
25 Switzerland, Swiss J. Geosci., 103(3), 363–374, doi:10.1007/s00015-010-0042-0, 2010.

Farley, K. A.: (U-Th)/He Dating: Techniques, Calibrations, and Applications, Rev. Mineral. Geochemistry, 47(1), 819–844, doi:10.2138/rmg.2002.47.18, 2002.

Farley, K. A., Wolf, R. A. and Silver, L. T.: The effects of long alpha-stopping distances on (U-Th)/He ages, Geochim. Cosmochim. Acta, 60(21), 4223–4229, doi:10.1016/S0016-7037(96)00193-7, 1996.

Frisch, W., Kuhlemann, J., Dunkl, I. and Brügel, A.: Palinspastic reconstruction and topographic evolution of the Eastern Alps during late Tertiary tectonic extrusion, Tectonophysics, 297(1–4), 1–15, doi:10.1016/S0040-1951(98)00160-7, 1998.

Fry, B., Deschamps, F., Kissling, E., Stehly, L. and Giardini, D.: Layered azimuthal anisotropy of Rayleigh wave phase velocities in the European Alpine lithosphere inferred from ambient noise, Earth Planet. Sci. Lett., 297(1–2), 95–102, doi:10.1016/j.epsl.2010.06.008, 2010.

Fuchs, W.: Gedanken zur Tektogenese der nördlichen Molasse zwischen Rhone und March, Jahrb. der Geol. Bundesanstalt, 119(2), 207–249, 1976.

Ganss, O. and Schmidt-Thomé, P.: Die gefaltete Molasse am Alpenrand zwischen Bodensee und Salzach, Zeitschrift der Dtsch. Geol. Gesellschaft, 105, 402–495, 1953.

Ganti, V., von Hagke, C., Scherler, D., Lamb, M. P., Fischer, W. W. and Avouac, J.-P.: Time scale bias in erosion rates of glaciated landscapes, Sci. Adv., 2(10), e1600204, doi:10.1126/sciadv.1600204, 2016.

Garefalakis, P. and Schlunegger, F.: Link between concentrations of sediment flux and deep crustal processes beneath the European Alps, Sci. Rep., 8(1), 183, doi:10.1038/s41598-017-17182-8, 2018.

Genser, J., Cloetingh, S. and Neubauer, F.: Late orogenic rebound and oblique Alpine convergence: New constraints from subsidence analysis of the Austrian Molasse basin, Glob. Planet. Change, 58(1–4), 214–223, doi:10.1016/j.gloplacha.2007.03.010, 2007.

Giamboni, M., Ustaszewski, K., Schmid, S. M., Schumacher, M. E. and Wetzel, A.: Plio-Pleistocene transpressional reactivation of Paleozoic and Paleogene structures in the Rhine-Bresse transform zone (northern Switzerland and eastern France), Int. J. Earth Sci., 93(2), 207–223, doi:10.1007/s00531-003-0375-2, 2004.

Giese, J., Seward, D., Stuart, F. M., Wüthrich, E., Gnos, E., Kurz, D., Eggenberger, U. and Schreurs, G.: Electrodynamic Disaggregation: Does it Affect Apatite Fission-Track and (U-Th)/He Analyses?, Geostand. Geoanalytical Res., 34(1), 39–48, doi:10.1111/j.1751-908X.2009.00013.x, 2010.

Glotzbach, C., Reinecker, J., Danišík, M., Rahn, M. K., Frisch, W. and Spiegel, C.: Thermal history of the central Gotthard and Aar massifs, European Alps: Evidence for steady state, long-term exhumation, J. Geophys. Res., 115, F03017, doi:10.1029/2009JF001304, 2010.

Guellec, S., Mugnier, J.-L., Tardy, M. and Roure, F.: Neogene evolution of the western Alpine foreland in the light of ECORS data and balanced cross-section, in Deep structure of the Alps, Mém. Soc. géol. suisse, vol. 1, edited by F. Roure, P. Heitzmann, and R. Polino, pp. 165–184, Société Geologique Suisse, Zürich., 1990.

Gusterhuber, J., Dunkl, I., Hinsch, R., Linzer, H.-G. and Sachsenhofer, R.: Neogene uplift and erosion in the Alpine Foreland Basin (Upper Austria and Salzburg), Geol. Carpathica, 63(4), 295–305, doi:10.2478/v10096-012-0023-5, 2012.

von Hagke, C. and Malz, A.: Triangle zones – Geometry, kinematics, mechanics, and the need for appreciation of uncertainties, Earth-Science Rev., 177(November 2017), 24–42, doi:10.1016/j.earscirev.2017.11.003, 2018.

von Hagke, C., Cederbom, C. E., Oncken, O., Stöckli, D. F., Rahn, M. K. and Schlunegger, F.: Linking the northern Alps with their foreland: The latest exhumation history resolved by low-temperature thermochronology, Tectonics, 31(5), TC5010, doi:10.1029/2011TC003078, 2012.

von Hagke, C., Oncken, O. and Evseev, S.: Critical taper analysis reveals lithological control of variations in detachment strength: An analysis of the Alpine basal detachment (Swiss Alps), Geochemistry, Geophys. Geosystems, 15(1), 176–191, doi:10.1002/2013GC005018, 2014a.

von Hagke, C., Oncken, O., Ortner, H., Cederbom, C. E. and Aichholzer, S.: Late Miocene to present deformation and erosion of the Central Alps — Evidence for steady state mountain building from thermokinematic data, Tectonophysics, 632, 250–260, doi:10.1016/j.tecto.2014.06.021, 2014b.

Haldemann, E. G., Haus, H. A., Holliger, A., Liechti, W., Rutsch, R. F. and della Valle, G.: Geological Atlas of Switzerland 1:25000, Map sheet Eggiwil (LK 1188), Federal Office of Topography swisstopo, Wabern, Switzerland., 1980.

Handy, M. R., Schmid, S. M., Bousquet, R., Kissling, E. and Bernoulli, D.: Reconciling plate-tectonic reconstructions of Alpine Tethys with the geological–geophysical record of spreading and subduction in the Alps, Earth-Science Rev., 102(3–4), 121–158, doi:10.1016/j.earscirev.2010.06.002, 2010.

Handy, M. R., Ustaszewski, K. and Kissling, E.: Reconstructing the Alps–Carpathians–Dinarides as a key to understanding switches in subduction polarity, slab gaps and surface motion, Int. J. Earth Sci., 104(1), 1–26, doi:10.1007/s00531-014-1060-3, 2015.

Haus, H.: Über alte Erosionserscheinungen am Südrand der miocaenen Nagelfluh des oberen Emmentales und deren Bedeutung für die Tektonik des Alpenrandes, Eclogae Geol. Helv., 28(2), 667–677, 1935.

Haus, H.: Geologie der Gegend von Schangnau im oberen Emmental (Kanton Bern): ein Beitrag zur Stratigraphie und Tektonik der subalpinen Molasse und des Alpenrandes, Beiträge zur Geol. Karte der Schweiz, NF 75, 106 pp., 1937.

Herwegh, M., Berger, A., Baumberger, R., Wehrens, P. and Kissling, E.: Large-Scale Crustal-Block-Extrusion During Late Alpine Collision, Sci. Rep., 7, 413, doi:10.1038/s41598-017-00440-0, 2017.

Herwegh, M., Berger, A., Glotzbach, C., Wangenheim, C., Mock, S., Wehrens, P., Baumberger, R., Egli, D. and Kissling, E.: Late Stages of Continent-Continent Collision: Timing, Kinematic Evolution, and Exhumation of the Northern Rim (Aar Massif) of the Alps, Earth Sci. Rev., n.d.

Hetényi, G., Molinari, I., Clinton, J., Bokelmann, G., Bondár, I., Crawford, W. C., Dessa, J.-X., Doubre, C., Friederich, W., Fuchs, F., Giardini, D., Gráczer, Z., Handy, M. R., Herak, M., Jia, Y., Kissling, E., Kopp, H., Korn, M., Margheriti, L., Meier,

T., Mucciarelli, M., Paul, A., Pesaresi, D., Piromallo, C., Plenefisch, T., Plomerová, J., Ritter, J., Rümpker, G., Šipka, V., Spallarossa, D., Thomas, C., Tilmann, F., Wassermann, J., Weber, M., Wéber, Z., Wesztergom, V. and Živčić, M.: The AlpArray Seismic Network: A Large-Scale European Experiment to Image the Alpine Orogen, Surv. Geophys., 39(5), 1009–1033, doi:10.1007/s10712-018-9472-4, 2018.

5   Hinsch, R.: Laterally varying structure and kinematics of the Molasse fold and thrust belt of the Central Eastern Alps: Implications for exploration, Am. Assoc. Pet. Geol. Bull., 97(10), 1805–1831, doi:l 0.1306/04081312129, 2013.

Homewood, P., Allen, P. A. and Williams, G. D.: Dynamics of the Molasse Basin of Western Switzerland, in Foreland Basins, pp. 199–217, Blackwell Publishing Ltd., Oxford, UK., 1986.

Hourigan, J. K., Reiners, P. W. and Brandon, M. T.: U-Th zonation-dependent alpha-ejection in (U-Th)/He chronometry,
10   Geochim. Cosmochim. Acta, 69(13), 3349–3365, doi:10.1016/j.gca.2005.01.024, 2005.

Hurford, A. J.: Cooling and uplift patterns in the Lepontine Alps South Central Switzerland and an age of vertical movement on the Insubric fault line, Contrib. to Mineral. Petrol., 92(4), 413–427, doi:10.1007/BF00374424, 1986.

Ji, W., Malusà, M. G., Tiepolo, M., Langone, A., Zhao, L. and Wu, F.: Synchronous Periadriatic magmatism in the Western and Central Alps in the absence of slab breakoff, Terra Nov., 31(2), 120–128, doi:10.1111/ter.12377, 2019.

15   Jordi, H. A.: Blatt 1188 Eggiwil, Geol. Atlas Schweiz 1 25 000, Erläut. 75, 2012.

Karner, G. D. and Watts, A. B.: Gravity anomalies and flexure of the lithosphere at mountain ranges, J. Geophys. Res. Solid Earth, 88(B12), 10449–10477, doi:10.1029/JB088iB12p10449, 1983.

Kästle, E. D., Rosenberg, C., Boschi, L., Bellahsen, N., Meier, T. and El-Sharkawy, A.: Slab Break-offs in the Alpine Subduction Zone, Solid Earth Discuss., (January), 1–16, doi:10.5194/se-2019-17, 2019.

20   Kempf, O., Matter, A., Burbank, D. W. and Mange, M.: Depositional and structural evolution of a foreland basin margin in a magnetostratigraphic framework: the eastern Swiss Molasse Basin, Int. J. Earth Sci., 88(2), 253–275, doi:10.1007/s005310050263, 1999.

Ketcham, R. A.: Forward and Inverse Modeling of Low-Temperature Thermochronometry Data, Rev. Mineral. Geochemistry, 58(1), 275–314, doi:10.2138/rmg.2005.58.11, 2005.

25   Kissling, E.: Deep structure and tectonics of the Valais - And the rest of the Alps, Bull. fuer Angew. Geol., 13(2), 3–10, 2008.

Kissling, E. and Schlunegger, F.: Rollback Orogeny Model for the Evolution of the Swiss Alps, Tectonics, 37(4), 1097–1115, doi:10.1002/2017TC004762, 2018.

Kissling, E., Schmid, S. M., Lippitsch, R., Ansorge, J. and Fügenschuh, B.: Lithosphere structure and tectonic evolution of the Alpine arc: new evidence from high-resolution teleseismic tomography, Geol. Soc. London, Mem., 32(1), 129–145,

doi:10.1144/GSL.MEM.2006.032.01.08, 2006.

Kuhlemann, J. and Kempf, O.: Post-Eocene evolution of the North Alpine Foreland Basin and its response to Alpine tectonics, Sediment. Geol., 152(1–2), 45–78, doi:10.1016/S0037-0738(01)00285-8, 2002.

Landesgeologie: Geological Map of Switzerland 1:500'000, Federal Office of Topography swisstopo, Wabern, Switzerland., 2005.

Laubscher, H. P.: Die Fernschubhypothese der Jurafaltung, Eclogae Geol. Helv., 54(1), 221–280, 1961.

Laubscher, H. P.: Jura kinematics and the Molasse Basin, Eclogae Geol. Helv., 85(3), 653–675, 1992.

Leary, R., Orme, D. A., Laskowski, A. K., DeCelles, P. G., Kapp, P., Carrapa, B. and Dettinger, M.: Along-strike diachroneity in deposition of the Kailas Formation in central southern Tibet: Implications for Indian slab dynamics, Geosphere, 12(4), 1198–1223, doi:10.1130/GES01325.1, 2016.

Lemcke, K.: Das Bayerische Alpenvorland vor der Eiszeit, Schweizerbart Science Publishers, Stuttgart, Germany., 1988.

Liniger, H.: Pliozän und Tektonik des Juragebirges, Eclogae Geol. Helv., 60(2), 407–490, 1967.

Lippitsch, R., Kissling, E. and Ansorge, J.: Upper mantle structure beneath the Alpine orogen from high-resolution teleseismic tomography, J. Geophys. Res., 108(B8), 2376, doi:10.1029/2002JB002016, 2003.

Madritsch, H., Schmid, S. M. and Fabbri, O.: Interactions between thin- and thick-skinned tectonics at the northwestern front of the Jura fold-and-thrust belt (eastern France), Tectonics, 27(5), TC5005, doi:10.1029/2008TC002282, 2008.

Mazurek, M., Hurford, A. J. and Leu, W.: Unravelling the multi-stage burial history of the Swiss Molasse Basin: integration of apatite fission track, vitrinite reflectance and biomarker isomerisation analysis, Basin Res., 18(1), 27–50, doi:10.1111/j.1365-2117.2006.00286.x, 2006.

Mitterbauer, U., Behm, M., Brückl, E., Lippitsch, R., Guterch, A., Keller, G. R., Koslovskaya, E., Rumpfhuber, E.-M. and Šumanovac, F.: Shape and origin of the East-Alpine slab constrained by the ALPASS teleseismic model, Tectonophysics, 510(1–2), 195–206, doi:10.1016/j.tecto.2011.07.001, 2011.

Mock, S. and Herwegh, M.: Tectonics of the central Swiss Molasse Basin: Post-Miocene transition to incipient thick-skinned tectonics?, Tectonics, 36(9), 1699–1723, doi:10.1002/2017TC004584, 2017.

Molnar, P., England, P. and Martinod, J.: Mantle dynamics, uplift of the Tibetan Plateau, and the Indian Monsoon, Rev. Geophys., 31(4), 357, doi:10.1029/93RG02030, 1993.

Mosar, J.: Present-day and future tectonic underplating in the western Swiss Alps: reconciliation of basement/wrench-faulting and décollement folding of the Jura and Molasse basin in the Alpine foreland, Earth Planet. Sci. Lett., 173(3), 143–155, doi:10.1016/S0012-821X(99)00238-1, 1999.

Mosbrugger, V., Utescher, T. and Dilcher, D. L.: Cenozoic continental climatic evolution of Central Europe, Proc. Natl. Acad. Sci., 102(42), 14964–14969, doi:10.1073/pnas.0505267102, 2005.

Müller, M., Nieberding, F. and Wanninger, A.: Tectonic style and pressure distribution at the northern margin of the Alps between Lake Constance and the River Inn, Geol. Rundschau, 77(3), 787–796, doi:10.1007/BF01830185, 1988.

5   Nussbaum, C.: Neogene tectonics and thermal maturity of sediments of the easternmost Southern Alps (Friuli area, Italy), Université de Neuchâtel., 2000.

Oncken, O., Hindle, D., Kley, J., Elger, K., Victor, P. and Schemmann, K.: Deformation of the Central Andean Upper Plate System — Facts, Fiction, and Constraints for Plateau Models, in The Andes. Frontiers in Earth Sciences, edited by O. Oncken, G. Chong, G. Franz, P. Giese, H.-J. Götze, V. A. Ramos, M. R. Strecker, and P. Wigger, pp. 3–27, Springer, Berlin Heidelberg.,

10   2006.

Ortner, H., Reiter, F. and Brandner, R.: Kinematics of the Inntal shear zone–sub-Tauern ramp fault system and the interpretation of the TRANSALP seismic section, Eastern Alps, Austria, Tectonophysics, 414(1–4), 241–258, doi:10.1016/j.tecto.2005.10.017, 2006.

Ortner, H., Aichholzer, S., Zerlauth, M., Pilser, R. and Fügenschuh, B.: Geometry, amount, and sequence of thrusting in the

15   Subalpine Molasse of western Austria and southern Germany, European Alps, Tectonics, 34(1), 1–30, doi:10.1002/2014TC003550, 2015.

Peresson, H. and Decker, K.: Far-field effects of Late Miocene subduction in the Eastern Carpathians: E-W compression and inversion of structures in the Alpine-Carpathian-Pannonian region, Tectonics, 16(1), 38–56, doi:10.1029/96TC02730, 1997.

Pfiffner, O. A.: Evolution of the North Alpine Foreland Basin in the Central Alps, in Foreland Basins, edited by P. A. Allen

20   and P. Homewood, pp. 219–228, Blackwell Publishing Ltd., Oxford, UK., 1986.

Pfiffner, O. A.: Geologie der Alpen, 1st ed., Haupt, Bern, Stuttgart, Wien., 2009.

Pfiffner, O. A.: Structural Map of the Helvetic Zone of the Swiss Alps, including Vorarlberg (Austria) and Haute Savoie (France), 1:100 000, edited by Federal Office of Topography swisstopo, Geol. Spec. Map, 128(Explanatory notes), 2011.

Pfiffner, O. A., Erard, P. F. and Stäuble, M.: Two cross sections through the Swiss Molasse Basin (lines E4-E6, W1, W7-

25   W10), in Deep structure of the Swiss Alps. Results of NRP 20, edited by O. A. Pfiffner, P. Lehner, P. Heitzmann, S. Mueller, and A. Steck, pp. 64–72, Birkhäuser, Basel, Boston, Berlin., 1997.

Philippe, Y., Colletta, B., Deville, E. and Mascle, A.: The Jura fold-and-thrust belt: a kinematic model based on map-balancing, in Peri Thetys Memoir 2: Structure and prospects of Alpine Basins and Forelands, edited by P. A. Ziegler and F. Horvàth, pp. 235–261, Muséum national d'Histoire naturelle, Paris., 1996.

Pippèrr, M. and Reichenbacher, B.: Late Early Miocene palaeoenvironmental changes in the North Alpine Foreland Basin, Palaeogeogr. Palaeoclimatol. Palaeoecol., 468, 485–502, doi:10.1016/j.palaeo.2017.01.002, 2017.

Qorbani, E., Bianchi, I. and Bokelmann, G.: Slab detachment under the Eastern Alps seen by seismic anisotropy, Earth Planet. Sci. Lett., 409, 96–108, doi:10.1016/j.epsl.2014.10.049, 2015.

5 Ratschbacher, L., Frisch, W., Linzer, H.-G. and Merle, O.: Lateral extrusion in the eastern Alps, PArt 2: Structural analysis, Tectonics, 10(2), 257–271, doi:10.1029/90TC02623, 1991.

Reiners, P. W. and Brandon, M. T.: Using Thermochronology to Understand Orogenic Erosion, Annu. Rev. Earth Planet. Sci., 34(1), 419–466, doi:10.1146/annurev.earth.34.031405.125202, 2006.

Rosenberg, C. L. and Berger, A.: On the causes and modes of exhumation and lateral growth of the Alps, Tectonics, 28(6),
10 TC6001, doi:10.1029/2008TC002442, 2009.

Rosenberg, C. L. and Kissling, E.: Three-dimensional insight into Central-Alpine collision: Lower-plate or upper-plate indentation?, Geology, 41(12), 1219–1222, doi:10.1130/G34584.1, 2013.

Rosenberg, C. L., Berger, A., Bellahsen, N. and Bousquet, R.: Relating orogen width to shortening, erosion, and exhumation during Alpine collision, Tectonics, 34(6), 1306–1328, doi:10.1002/2014TC003736, 2015.

15 Rosenberg, C. L., Schneider, S., Scharf, A., Bertrand, A., Hammerschmidt, K., Rabaute, A. and Brun, J.-P.: Relating collisional kinematics to exhumation processes in the Eastern Alps, Earth-Science Rev., 176(October 2017), 311–344, doi:10.1016/j.earscirev.2017.10.013, 2018.

Rutsch, R.: Molasse und Quartär im Gebiet des Siegfriedblattes Rüeggisberg (Kanton Bern), Beiträge zur Geol. Karte der Schweiz, NF 87, 89 pp., 1947.

20 Schegg, R. and Leu, W.: Analysis of erosion events and palaeogeothermal gradients in the North Alpine Foreland Basin of Switzerland, Geol. Soc. London, Spec. Publ., 141(1), 137–155, doi:10.1144/GSL.SP.1998.141.01.09, 1998.

Schlunegger, F. and Castelltort, S.: Immediate and delayed signal of slab breakoff in Oligo/Miocene Molasse deposits from the European Alps, Sci. Rep., 6, 31010, doi:10.1038/srep31010, 2016.

Schlunegger, F. and Kissling, E.: Slab rollback orogeny in the Alps and evolution of the Swiss Molasse basin, Nat. Commun.,
25 6, 8605, doi:10.1038/ncomms9605, 2015.

Schlunegger, F. and Mosar, J.: The last erosional stage of the Molasse Basin and the Alps, Int. J. Earth Sci., 100(5), 1147–1162, doi:10.1007/s00531-010-0607-1, 2011.

Schlunegger, F. and Norton, K. P.: Headward retreat of streams in the Late Oligocene to Early Miocene Swiss Alps, edited by K. Föllmi, Sedimentology, 60(1), 85–101, doi:10.1111/sed.12010, 2013.

Schlunegger, F. and Norton, K. P.: Climate vs. tectonics: the competing roles of Late Oligocene warming and Alpine orogenesis in constructing alluvial megafan sequences in the North Alpine foreland basin, Basin Res., 27(2), 230–245, doi:10.1111/bre.12070, 2015.

Schlunegger, F. and Simpson, G.: Possible erosional control on lateral growth of the European Central Alps, Geology, 30(10), 907, doi:10.1130/0091-7613(2002)030<0907:PECOLG>2.0.CO;2, 2002.

Schlunegger, F., Matter, A. and Mange, M. A.: Alluvial fan sedimentation and structure of the southern Molasse Basin margin, Lake Thun area, Switzerland, Eclogae Geol. Helv., 86(3), 717–750, 1993.

Schlunegger, F., Burbank, D. W., Matter, A., Engesser, B. and Mödden, C.: Magnetostratigraphic calibration of the Oligocene to Middle Miocene (30-15 Ma) mammal biozones and depositional sequences of the Swiss Molasse Basin, Eclogae Geol. Helv., 89, 753–788, 1996.

Schlunegger, F., Matter, A., Burbank, D. W. and Klaper, E. M.: Magnetostratigraphic constraints on relationships between evolution of the central Swiss Molasse basin and Alpine orogenic events, Geol. Soc. Am. Bull., 109(2), 225–241, doi:10.1130/0016-7606(1997)109<0225:MCORBE>2.3.CO;2, 1997.

Schlunegger, F., Rieke-Zapp, D. and Ramseyer, K.: Possible environmental effects on the evolution of the Alps-Molasse Basin system, Swiss J. Geosci., 100(3), 383–405, doi:10.1007/s00015-007-1238-9, 2007.

Schlunegger, F., Anspach, O., Bieri, B., Böning, P., Kaufmann, Y., Lahl, K., Lonschinski, M., Mollet, H., Sachse, D., Schubert, C., Stöckli, G. and Zander, I.: Geological Atlas of Switzerland 1:25000, Map sheet Schüpfheim (LK 1169), Federal Office of Topography swisstopo, Wabern, Switzerland., 2016.

Schmid, S. M., Pfiffner, O. A., Froitzheim, N., Schönborn, G. and Kissling, E.: Geophysical-geological transect and tectonic evolution of the Swiss-Italian Alps, Tectonics, 15(5), 1036–1064, doi:10.1029/96TC00433, 1996.

Schmid, S. M., Fügenschuh, B., Kissling, E. and Schuster, R.: Tectonic map and overall architecture of the Alpine orogen, Eclogae Geol. Helv., 97(1), 93–117, doi:10.1007/s00015-004-1113-x, 2004.

Schmid, S. M., Kissling, E., Diehl, T., van Hinsbergen, D. J. J. and Molli, G.: Ivrea mantle wedge, arc of the Western Alps, and kinematic evolution of the Alps–Apennines orogenic system, Swiss J. Geosci., 110(2), 581–612, doi:10.1007/s00015-016-0237-0, 2017.

Schönborn, G.: Alpine tectonics and kinematic models of the central Southern Alps, Mem. di Sci. Geol. Padova, 44, 229–393, 1992.

Schuller, V., Frisch, W. and Herzog, U.: Critical taper behaviour and out-of-sequence thrusting on orogenic wedges - an example of the Eastern Alpine Molasse Basin, Terra Nov., 27(3), 231–237, doi:10.1111/ter.12152, 2015.

Schwartz, S., Gautheron, C., Audin, L., Dumont, T., Nomade, J., Barbarand, J., Pinna-Jamme, R. and van der Beek, P.: Foreland exhumation controlled by crustal thickening in the Western Alps, Geology, 45(2), 139–142, doi:10.1130/G38561.1, 2017.

Sinclair, H. D.: Flysch to molasse transition in peripheral foreland basins: The role of the passive margin versus slab breakoff, Geology, 25(12), 1123, doi:10.1130/0091-7613(1997)025<1123:FTMTIP>2.3.CO;2, 1997.

Sinclair, H. D. and Allen, P. A.: Vertical versus horizontal motions in the Alpine orogenic wedge: stratigraphic response in the foreland basin, Basin Res., 4(3–4), 215–232, doi:10.1111/j.1365-2117.1992.tb00046.x, 1992.

Sinclair, H. D., Coakley, B. J., Allen, P. A. and Watts, A. B.: Simulation of Foreland Basin Stratigraphy using a diffusion model of mountain belt uplift and erosion: An example from the central Alps, Switzerland, Tectonics, 10(3), 599–620, doi:10.1029/90TC02507, 1991.

Sommaruga, A.: Décollement tectonics in the Jura forelandfold-and-thrust belt, Mar. Pet. Geol., 16(2), 111–134, doi:10.1016/S0264-8172(98)00068-3, 1999.

Sommaruga, A., Eichenberger, U. and Marillier, F.: Seismic Atlas of the Swiss Molasse Basin, edited by the Swiss Geophysical Commission, Matériaux pour la Géologie la Suisse - Géophysique, (44), 2012.

Spiegel, C., Kuhlemann, J., Dunkl, I. and Frisch, W.: Paleogeography and catchment evolution in a mobile orogenic belt: the Central Alps in Oligo–Miocene times, Tectonophysics, 341(1–4), 33–47, doi:10.1016/S0040-1951(01)00187-1, 2001.

Stäuble, M. and Pfiffner, O. A.: Processing, interpretation and modeling of seismic reflection data in the Molasse Basin of eastern Switzerland, Eclogae Geol. Helv., 84(1), 151–175, doi:10.5169/seals-166767, 1991.

Strunck, P. and Matter, A.: Depositional evolution of the western Swiss Molasse, Eclogae Geol. Helv., 95(2), 197–222, doi:http://dx.doi.org/10.5169/seals-168955, 2002.

Ustaszewski, K. and Schmid, S. M.: Latest Pliocene to recent thick-skinned tectonics at the Upper Rhine Graben – Jura Mountains junction, Swiss J. Geosci., 100(2), 293–312, doi:10.1007/s00015-007-1226-0, 2007.

Valla, P. G., van der Beek, P. A., Shuster, D. L., Braun, J., Herman, F., Tassan-Got, L. and Gautheron, C.: Late Neogene exhumation and relief development of the Aar and Aiguilles Rouges massifs (Swiss Alps) from low-temperature thermochronology modeling and 4 He/ 3 He thermochronometry, J. Geophys. Res. Earth Surf., 117, F01004, doi:10.1029/2011JF002043, 2012.

Vermeesch, P.: Three new ways to calculate average (U–Th)/He ages, Chem. Geol., 249(3–4), 339–347, doi:10.1016/j.chemgeo.2008.01.027, 2008.

Vernon, A. J., van der Beek, P. A., Sinclair, H. D., Persano, C., Foeken, J. and Stuart, F. M.: Variable late Neogene exhumation

of the central European Alps: Low-temperature thermochronology from the Aar Massif, Switzerland, and the Lepontine Dome, Italy, Tectonics, 28(5), TC5004, doi:10.1029/2008TC002387, 2009.

Vollmayr, T.: Strukturelle Ergebnisse der Kohlenwasserstoffexploration im Gebiet von Thun, Schweiz, Eclogae Geol. Helv., 85(3), 531–539, 1992.

5   Wehrens, P., Baumberger, R., Berger, A. and Herwegh, M.: How is strain localized in a meta-granitoid, mid-crustal basement section? Spatial distribution of deformation in the central Aar massif (Switzerland), J. Struct. Geol., 94, 47–67, doi:10.1016/j.jsg.2016.11.004, 2017.

Weidmann, M., Homewood, P., Morel, R., Berchten, J.-D., Bucher, H., Burri, M., Cornioley, J.-D., Escher, P., Rück, P., Tabotta, A. and Zahner, P.: Geological Atlas of Switzerland 1:25000, Map sheet Châtel-St-Denis (LK 1244), Federal Office
10 of Topography swisstopo, Wabern, Switzerland., 1993.

Weisenberger, T. B., Rahn, M. K., van der Lelij, R., Spikings, R. A. and Bucher, K.: Timing of low-temperature mineral formation during exhumation and cooling in the Central Alps, Switzerland, Earth Planet. Sci. Lett., 327–328, 1–8, doi:10.1016/j.epsl.2012.01.007, 2012.

Whipple, K. X.: The influence of climate on the tectonic evolution of mountain belts, Nat. Geosci., 2(2), 97–104,
15 doi:10.1038/ngeo413, 2009.

Willett, S. D. and Schlunegger, F.: The last phase of deposition in the Swiss Molasse Basin: from foredeep to negative-alpha basin, Basin Res., 22(5), 623–639, doi:10.1111/j.1365-2117.2009.00435.x, 2010.

Willett, S. D., Schlunegger, F. and Picotti, V.: Messinian climate change and erosional destruction of the central European Alps, Geology, 34(8), 613, doi:10.1130/G22280.1, 2006.

20 Wolf, R. A., Farley, K. A. and Silver, L. T.: Helium diffusion and low-temperature thermochronometry of apatite, Geochim. Cosmochim. Acta, 60(21), 4231–4240, doi:10.1016/S0016-7037(96)00192-5, 1996.

Zaugg, A., Löpfe, R., Kriemler, M. and Kempf, T.: Geological Atlas of Switzerland 1:25000, Federal Office of Topography swisstopo, Wabern, Switzerland., 2011.

Zhao, L., Paul, A., Malusà, M. G., Xu, X., Zheng, T., Solarino, S., Guillot, S., Schwartz, S., Dumont, T., Salimbeni, S., Aubert,
25 C., Pondrelli, S., Wang, Q. and Zhu, R.: Continuity of the Alpine slab unraveled by high-resolution P wave tomography, J. Geophys. Res. Solid Earth, 121(12), 8720–8737, doi:10.1002/2016JB013310, 2016.

Zweigel, J., Aigner, T., Luterbacher, H., Fleet, A. J., Morton, A. C. and Roberts, A. M.: Eustatic versus tectonic controls on Alpine foreland basin fill: sequence stratigraphy and subsidence analysis in the SE German molasse, Cenozoic Forel. basins West. Eur., 134, 299–324, doi:10.1144/GSL.SP.1998.134.01.14, 1998.

Table 1 Apatite (U-Th-Sm)/He dating results

Sample	He vol. [ncc][a]	1σ [%]	U mass [ng]	1σ [%]	Th mass [ng]	1σ [%]	Sm mass [ng]	1σ [%]	Ft[b]	Raw age [Ma]	Corrected age [Ma]	2σ [Ma][c]	Average age [Ma][d]	2 std. error [Ma][e]	Excluded age[f]
SM-1 a1	0.02	3.77	0.01	5.64	0.07	2.56	0.34	7.06	0.60	5.5	9.0	1.4			
SM-1 a2	0.08	2.09	0.04	2.66	0.21	2.45	0.98	6.92	0.72	7.2	10.0	1.0			
SM-1 a4	0.07	2.43	0.03	3.18	0.15	2.47	0.66	6.84	0.74	8.5	11.5	1.2			
SM-1 a5	0.03	3.70	0.02	4.97	0.07	2.56	0.40	7.15	0.69	6.2	9.0	1.2			
SM-1 a6	0.08	2.09	0.03	2.52	0.15	2.45	0.55	3.47	0.68	9.4	13.9	1.5			
SM-1 a7	0.05	2.67	0.02	3.25	0.14	2.46	0.92	3.64	0.79	6.9	8.8	0.8			
SM-1 a8	0.04	3.24	0.03	2.65	0.02	2.82	0.23	3.34	0.64	8.1	12.6	1.7	10.7	0.8	
SM-4 a1	0.03	3.13	0.02	3.08	0.01	2.48	0.03	3.70	0.66	10.5	15.9	2.1			e
SM-4 a2	0.06	2.51	0.06	2.03	0.10	2.42	0.37	3.70	0.61	5.9	9.6	1.2			
SM-4 a3	0.01	4.81	0.02	3.79	0.05	2.49	0.56	3.70	0.59	3.0	5.0	0.8			e
SM-4 a4	0.06	2.64	0.05	2.20	0.06	2.45	0.51	3.70	0.61	6.6	10.8	1.4			
SM-4 a5	0.02	4.31	0.02	3.99	0.03	2.54	0.34	3.70	0.55	5.0	9.2	1.5			
SM-4 a6	0.08	2.21	0.07	2.01	0.02	2.64	0.38	3.70	0.66	8.6	13.1	1.5	10.7	0.9	
SM-5 a1	0.05	2.79	0.04	2.52	0.13	2.46	0.90	3.70	0.62	4.7	7.5	1.0			
SM-5 a2	0.10	2.11	0.15	1.86	0.09	2.43	0.66	3.70	0.66	4.6	7.0	0.8			
SM-5 a3	0.02	4.42	0.02	4.25	0.06	2.57	0.25	3.70	0.74	4.3	5.8	0.7			
SM-5 a4	0.01	5.90	0.01	6.10	0.09	2.50	0.22	3.70	0.62	2.2	3.6	0.6			e
SM-5 a5	0.04	3.02	0.04	2.35	0.15	2.46	1.00	3.70	0.65	3.7	5.6	0.7			
SM-5 a6	0.20	1.51	0.13	1.88	0.08	2.44	0.54	3.70	0.63	11.3	18.1	2.2	6.5	0.5	e
SM-6 a1	0.05	2.66	0.05	2.20	0.10	2.43	0.83	3.70	0.61	6.0	9.8	1.3			
SM-6 a2	0.07	2.20	0.07	2.04	0.12	2.47	1.30	3.70	0.82	5.6	6.8	0.5			
SM-6 a3	0.04	2.90	0.04	2.29	0.08	2.44	0.77	3.70	0.61	4.8	7.8	1.1			
SM-6 a4	0.00	9.84	0.00	43.45	0.01	2.77	1.05	3.70	0.59	0.8	1.3	0.4			e
SM-6 a5	0.14	1.72	0.13	1.87	0.02	2.68	0.51	3.70	0.64	7.9	12.3	1.4	9.2	1.2	
SM-7 a1	0.01	7.55	0.01	5.93	0.03	2.67	0.34	4.55	0.54	2.1	3.9	0.8			e
SM-7 a2	0.03	3.57	0.02	3.57	0.02	2.88	0.43	3.21	0.69	7.9	11.5	1.5			
SM-7 a3	0.15	1.66	0.07	2.00	0.07	2.52	0.31	4.06	0.62	13.5	21.7	2.7			
SM-7 a4	0.02	4.43	0.02	4.16	0.04	2.62	0.31	3.52	0.57	5.1	9.0	1.5			
SM-7 a5	0.05	2.85	0.03	2.82	0.05	2.58	0.41	3.81	0.54	8.4	15.7	2.4			
SM-7 a6	0.02	4.37	0.02	3.98	0.05	2.45	0.57	3.70	0.71	3.7	5.2	0.7			e
SM-7 a7	0.02	4.28	0.01	6.31	0.04	2.65	0.60	3.70	0.65	6.1	9.5	1.4			
SM-7 a8	0.24	1.48	0.13	1.87	0.11	2.42	0.57	3.70	0.73	12.3	16.9	1.6			
SM-7 a9	0.00	8.62	0.00	28.40	0.03	2.69	0.30	3.70	0.55	2.4	4.3	1.1			e
SM-8 a1	0.02	3.67	0.02	3.39	0.06	2.54	0.56	4.01	0.77	4.4	5.7	0.6			
SM-8 a2	0.02	3.68	0.03	3.02	0.03	2.67	0.43	4.57	0.70	4.7	6.8	0.8			
SM-8 a3	0.12	1.93	0.03	2.61	0.08	2.50	0.56	3.86	0.77	18.5	24.0	2.1			e
SM-8 a4	0.02	3.88	0.02	3.25	0.06	2.55	0.53	3.32	0.80	4.5	5.6	0.6	6.0	0.4	
SM-11 a1	0.05	2.53	0.05	2.14	0.11	2.42	0.47	4.56	0.78	5.5	7.0	0.6			
SM-11 a2	0.02	4.35	0.02	3.89	0.06	2.45	0.34	3.42	0.73	5.3	7.2	0.9			
SM-11 a3	0.02	4.04	0.02	4.02	0.07	2.43	0.52	3.68	0.75	4.1	5.6	0.7			
SM-11 a4	0.02	4.77	0.02	3.77	0.06	2.44	0.30	4.20	0.57	3.8	6.6	1.1			
SM-11 a5	0.05	2.52	0.04	2.35	0.04	2.49	0.26	4.54	0.67	9.2	13.6	1.6	6.6	0.4	e
SM-12 a1	0.04	3.00	0.04	2.22	0.06	2.44	0.40	3.80	0.51	5.5	10.7	1.7			
SM-12 a2	0.26	1.50	0.15	1.84	0.01	2.72	0.46	4.13	0.69	13.4	19.4	2.0			e
SM-12 a3	0.02	3.63	0.03	2.85	0.03	2.51	0.36	3.46	0.74	5.4	7.3	0.8			
SM-12 a4	0.22	1.50	0.19	1.83	0.18	2.41	0.46	4.07	0.82	7.8	9.6	0.7	9.2	1.0	
SM-13 a1	0.06	2.27	0.07	1.99	0.02	2.84	0.59	3.13	0.61	6.1	10.0	1.3			

Sample	He vol. [ncc][a]	1σ [%]	U mass [ng]	1σ [%]	Th mass [ng]	1σ [%]	Sm mass [ng]	1σ [%]	Ft[b]	Raw age [Ma]	Corrected age [Ma]	2σ [Ma][c]	Average age [Ma][d]	2 std. error [Ma][e]	Excluded age[f]
SM-13 a2	0.04	2.93	0.03	2.54	0.04	2.67	0.39	3.93	0.68	6.6	9.7	1.2			
SM-13 a3	0.06	2.59	0.07	2.05	0.01	3.46	0.35	4.68	0.74	6.8	9.1	0.9			
SM-13 a4	0.02	4.51	0.02	2.96	0.02	2.71	0.31	4.28	0.63	4.3	6.9	1.0			
SM-13 a5	0.01	6.37	0.01	5.91	0.01	2.82	0.34	3.96	0.76	3.2	4.2	0.7	8.9	0.7	e
SM-14 a1	0.06	2.60	0.03	2.71	0.06	2.44	0.55	3.70	0.68	8.9	13.0	1.5			e
SM-14 a2	0.03	3.33	0.02	3.21	0.07	2.44	0.39	3.70	0.56	6.4	11.4	1.7			
SM-14 a3	0.05	2.66	0.03	2.70	0.10	2.48	0.32	3.70	0.59	6.8	11.4	1.6			
SM-14 a4	0.02	4.41	0.02	3.66	0.05	2.62	1.11	3.70	0.61	3.4	5.7	0.9			e
SM-14 a5	0.04	3.07	0.02	3.59	0.07	2.53	0.41	3.70	0.73	7.1	9.7	1.1			
SM-14 a6	0.07	2.25	0.05	2.10	0.09	2.43	2.20	3.70	0.79	6.5	8.3	0.7	10.8	0.6	e
SM-15 a1	0.04	2.72	0.04	2.44	0.18	2.41	2.39	3.70	0.71	3.5	5.0	0.5			
SM-15 a2	0.11	1.82	0.05	2.33	0.12	2.42	0.39	3.70	0.66	12.2	18.4	2.1			e
SM-15 a3	0.04	2.92	0.04	2.60	0.17	2.41	0.82	3.70	0.64	3.7	5.8	0.7			
SM-15 a4	0.46	1.26	0.16	1.85	0.77	2.41	0.62	3.70	0.76	11.1	14.5	1.2			e
SM-15 a5	0.03	3.24	0.03	2.87	0.08	2.50	0.51	3.70	0.61	4.0	6.5	0.9			
SM-15 a6	0.08	2.13	0.07	2.16	0.17	2.42	2.56	3.70	0.69	4.8	7.0	0.8	6.1	0.4	
SM-16 a1	0.27	1.33	0.09	1.96	0.09	2.43	3.15	3.70	0.71	16.6	23.5	2.3			
SM-16 a2	0.90	1.01	0.36	1.82	0.28	2.41	1.98	3.70	0.73	16.9	23.2	2.1			
SM-16 a3	0.25	1.56	0.12	1.87	0.18	2.41	0.37	3.70	0.72	12.5	17.3	1.6			e
SM-16 a4	0.01	6.40	0.01	7.86	0.06	2.46	0.28	3.70	0.75	3.3	4.3	0.7			e
SM-16 a5	0.14	1.77	0.18	1.84	0.03	2.52	1.03	3.70	0.76	6.0	7.9	0.7			
SM-16 a7	0.04	3.25	0.09	1.90	0.07	2.44	0.55	3.70	0.69	3.1	4.4	0.5			e

[a]Amount of helium is given in nano-cubic-cm in standard temperature and pressure.

[b]Ejection correction (Ft): correction factor for alpha-ejection (Farley et al., 1996; Hourigan et al., 2005).

[c]Uncertaintiy of the single grain age is given as 2 sigma in % (or in Ma) and it includs both the analytical uncertainty and the estimated uncertainty of the Ft.

[d]Average ages for totally reset samples were calculated as the unweighted arithmetic mean.

[g]Uncertainty of the sample average age is 2 standard error, as (SD)/(n)1/2; where SD=standard deviation of the age replicates and n=number of age determinations.

[f]Ages with a substantial first He re-extract (> 4%) and/or a total analytical error of > 10% have been excluded. Outliers on the [He]–P plot have also been excluded (Vermeesch, 2008).
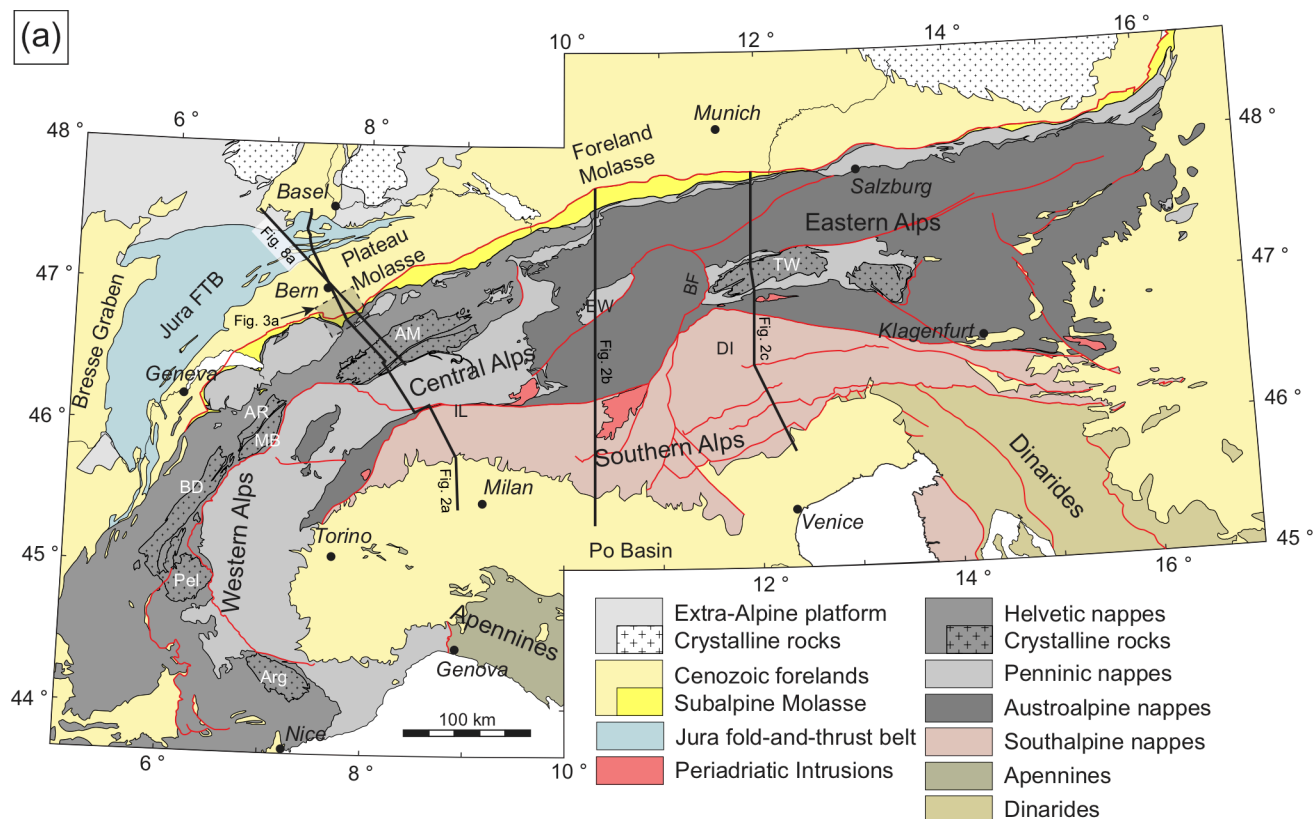
Fig. 1 (a) Tectonic map of the European Alps and its foreland basins (adapted from Schmid et al., 2004). Traces of the cross-sections in Fig. 2 and Fig. 8a are given as bold black lines. The sample area south of Bern (Fig. 3a) is denoted by a dashed rectangle. AM, Aar Massif; AR, Aiguilles-Rouges Massif; BD, Belledonne Massif; BF, Brenner Fault; DI, Dolomite indenter; EW, Engadine Window; FTB, fold-and-thrust belt; IL, Insubric Line; MB, Mont-Blanc Massif; Pel, Pelvoux Massif; TW, Tauern Window
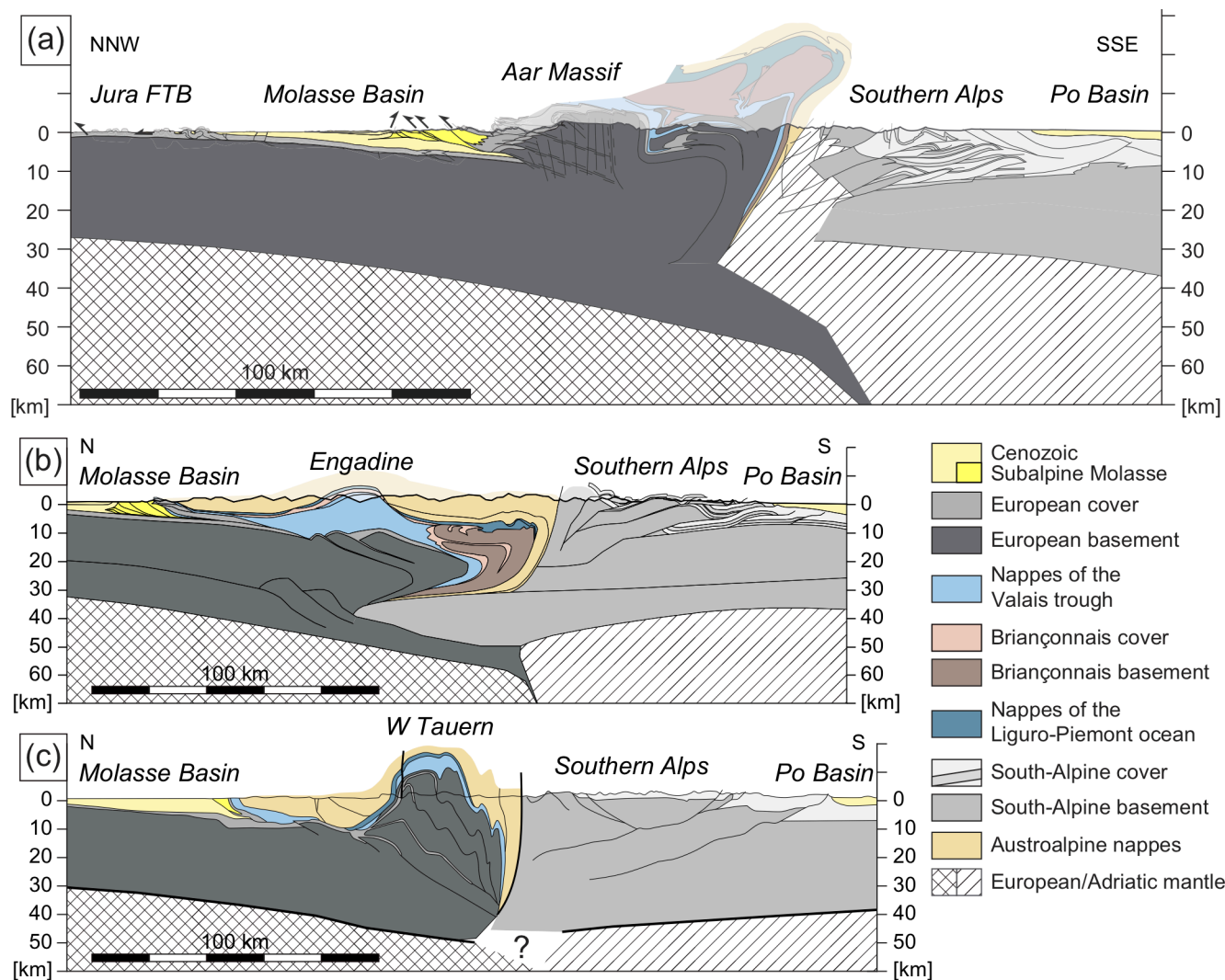
Fig. 2 Cross-sections through the Alps. (a) Jura - Plateau Molasse - Aar Massif (compiled from Buxtorf, 1916; Herwegh et al., 2017; Mock and Herwegh, 2017; Pfiffner, 2009; Rosenberg and Kissling, 2013). (b) Engadine Window (adapted from Rosenberg et al., 2015). (c) Western Tauern Window (adapted from Rosenberg et al., 2015).
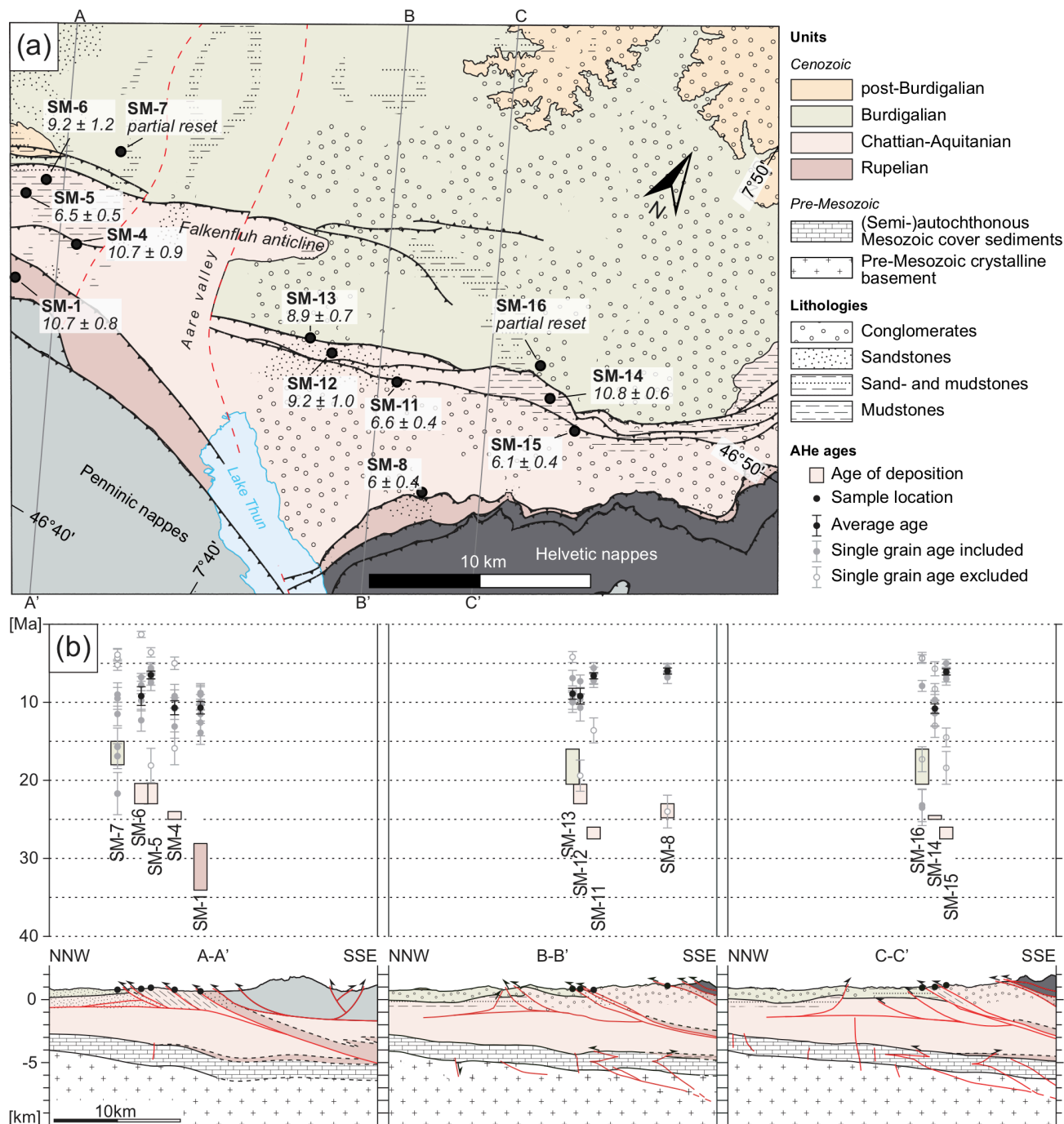
Fig. 3 (a) Litho-tectonic map of the Lake Thun area showing sample locations and corresponding average apatite (U-Th-Sm)/He (AHe) ages. Traces of cross-sections A-A', B-B', and C-C' in Fig. 3b are given as black lines. The location of the sampling area is shown as a dashed rectangle in Fig. 1. Note the arrow indicating north. (b) Cross-sections through the sampling area west (A-A') and east of the Aare valley (B-B' and C-C'), showing single grain and average AHe ages

West **East** **North**

no solution!

South

- Post-depositional cooling history
- Envelope of acceptable paths (goodness-of-fit ≥ 0.05)
- Good paths (goodness-of-fit ≥ 0.5)
- Thrust
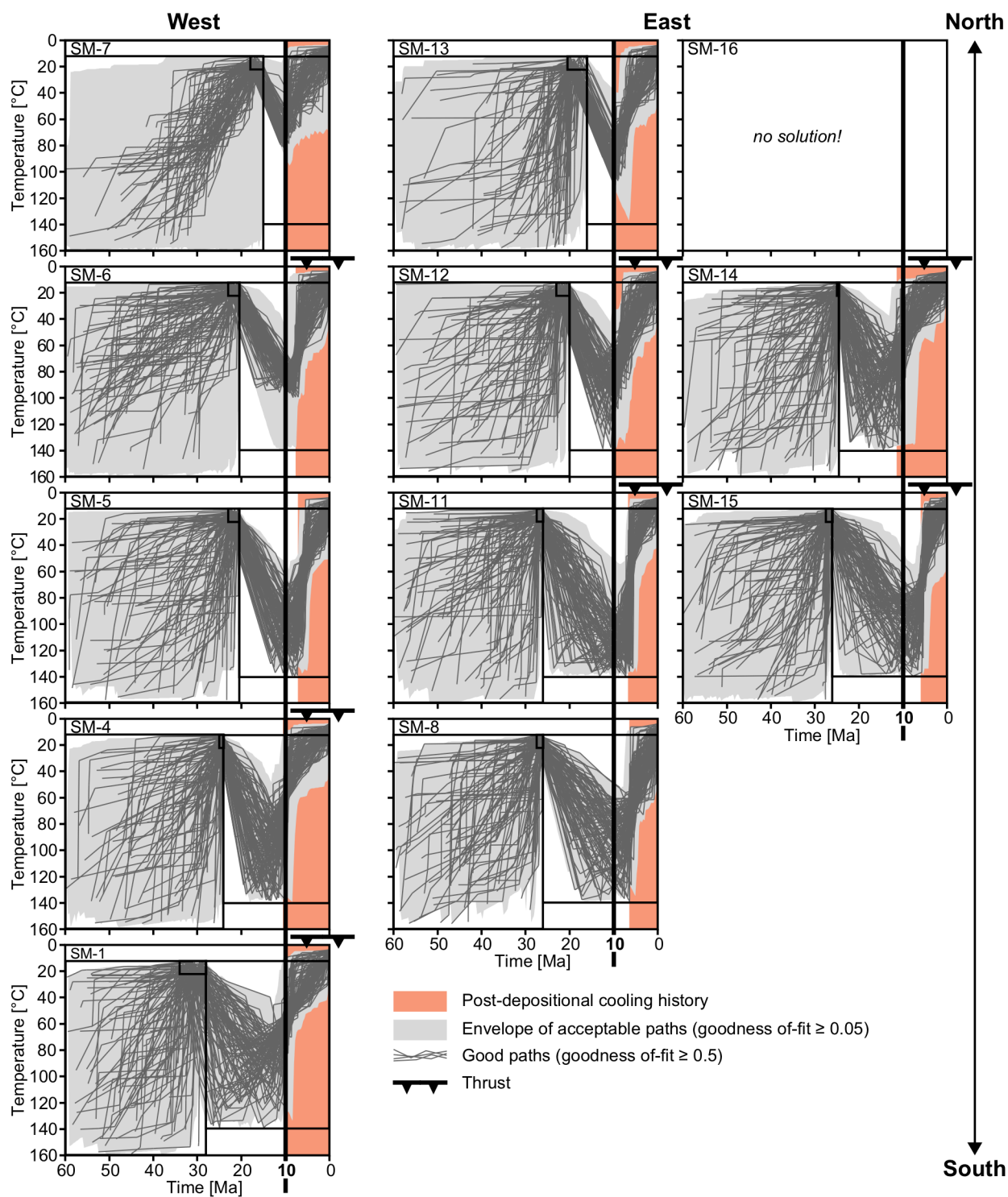
Fig. 4 Thermal evolution of samples. The results from inverse modeling of apatite (U-Th-Sm)/He (AHe) ages with the HeFTy software (Ketcham, 2005) show the time-temperature history of the samples discussed in the text. Modeling constraints are shown as black boxes. The bold black lines at 10 Ma serve as a visual time reference. The thermal histories for the different

5 samples are aligned from north to south and from east to west according to their sample location
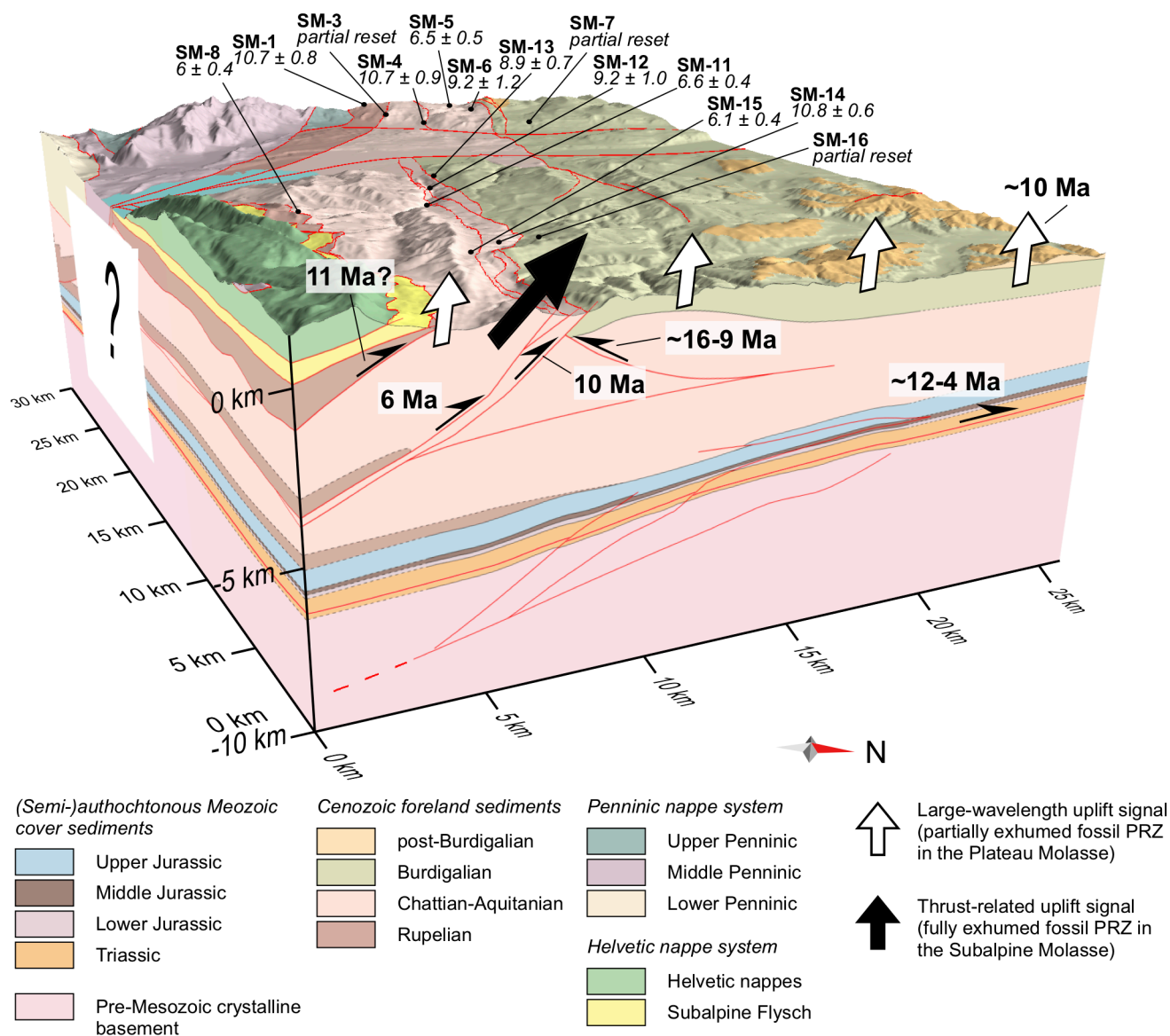
Fig. 5 Block model of with sample locations and corresponding average (U-Th-Sm)/He ages. The construction of the block model is based on surface (Beck, 1945; Haus, 1937; Jordi, 2012; Rutsch, 1947; Schlunegger et al., 1993, 1997) and subsurface (2D seismic interpretation; Mock and Herwegh, 2017) geological information. PRZ, partial retention zone

Tectonic units

Extra-Alpine platform	Jura fold-and-thrust belt
Crystalline rocks	Helvetic nappes
Cenozoic forelands	Crystalline rocks
Plateau/Foreland Molasse	Penninic nappes
Subalpine Molasse	Austroalpine / Southalpine nappes

AHe ages

★ this study
▲ von Hagke et al. (2012)
◆ von Hagke et al. (2014)

Thrust activity

Ortner et al. (2015)

Late Miocene shortening estimates

1: Philippe et al. (1996)
2: Burkhard and Sommaruga (1998)
3: this study
4: von Hagke et al. (2012)
5: von Hagke et al. (2014), Ortner et al. (2015)
6: Ortner et al. (2015)

Fig. 6 Along-strike variations in late Miocene deformation of the North Alpine foreland between Lake Geneva and Salzburg. (a) Tectonic map (modified from Schmid et al., 2004) and activity of thrusting in the Subalpine Molasse deduced from AHe ages and geological interpretation. (b) Tectonic map (modified from Schmid et al., 2004) and estimated amount of late Miocene shortening in the North Alpine foreland (i.e., Subalpine Molasse, and Jura FTB). Estimates from the Subalpine Molasse record minimum shortening. (c) Top basement map of the Central Alps (modified from Pfiffner, 2011) showing the highly non-cylindrical hinterland architecture with the high relief domains of the External Crystalline Massifs (ECMs). Red arrows indicate the constant late Miocene deformation signal with a slight decrease in horizontal shortening recorded in the North Alpine foreland. AM, Aar Massif; AR, Aiguilles-Rouges Massif; BD, Belledonne Massif; EW, Engadine Window; MB, Mont-Blanc Massif; TW, Tauern Window
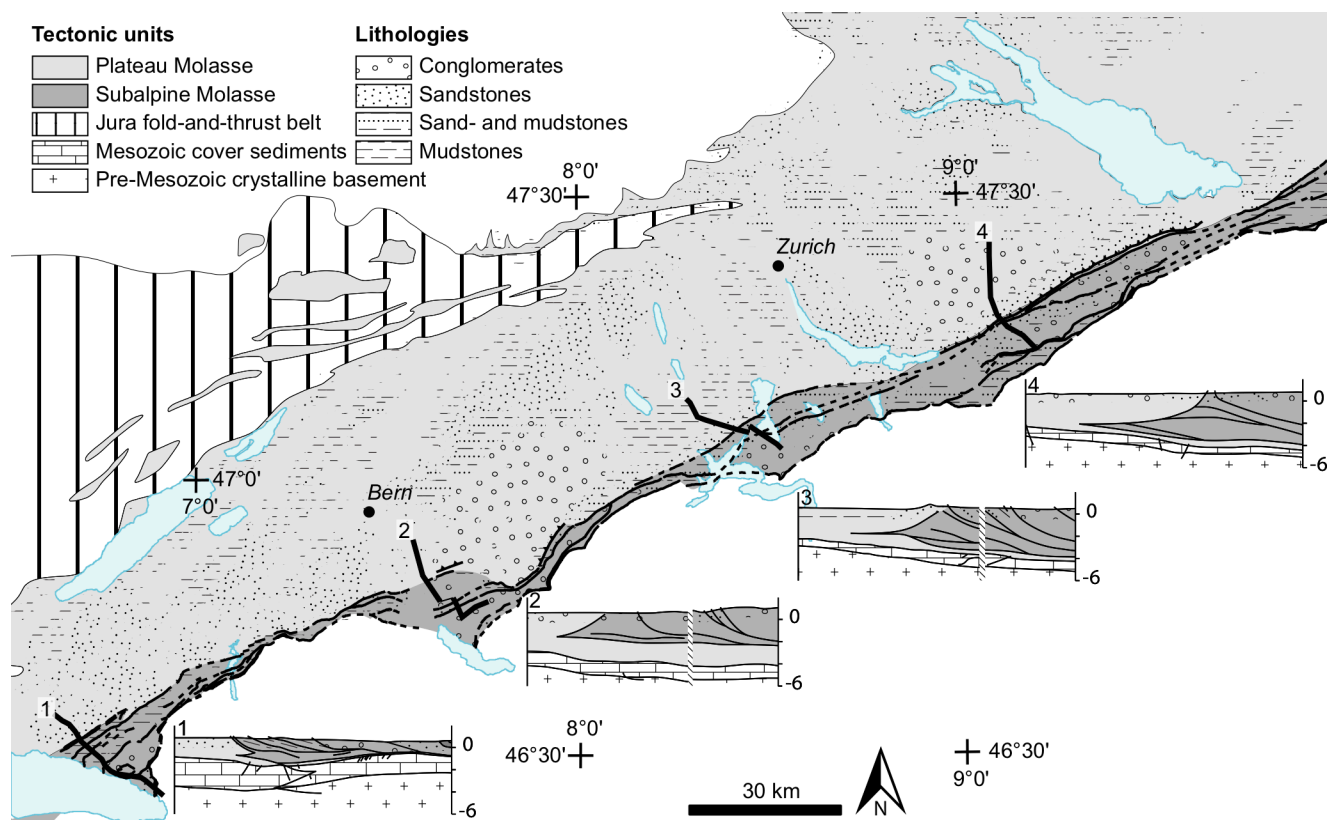
Fig. 7 Litho-tectonic map of the Swiss Molasse Basin (modified from Landesgeologie, 2005). Cross-sections 1-4 are based on 2D seismic interpretation (cross-section 2, Mock and Herwegh, 2017; cross-sections 1, 3, and 4, Sommaruga et al., 2012)
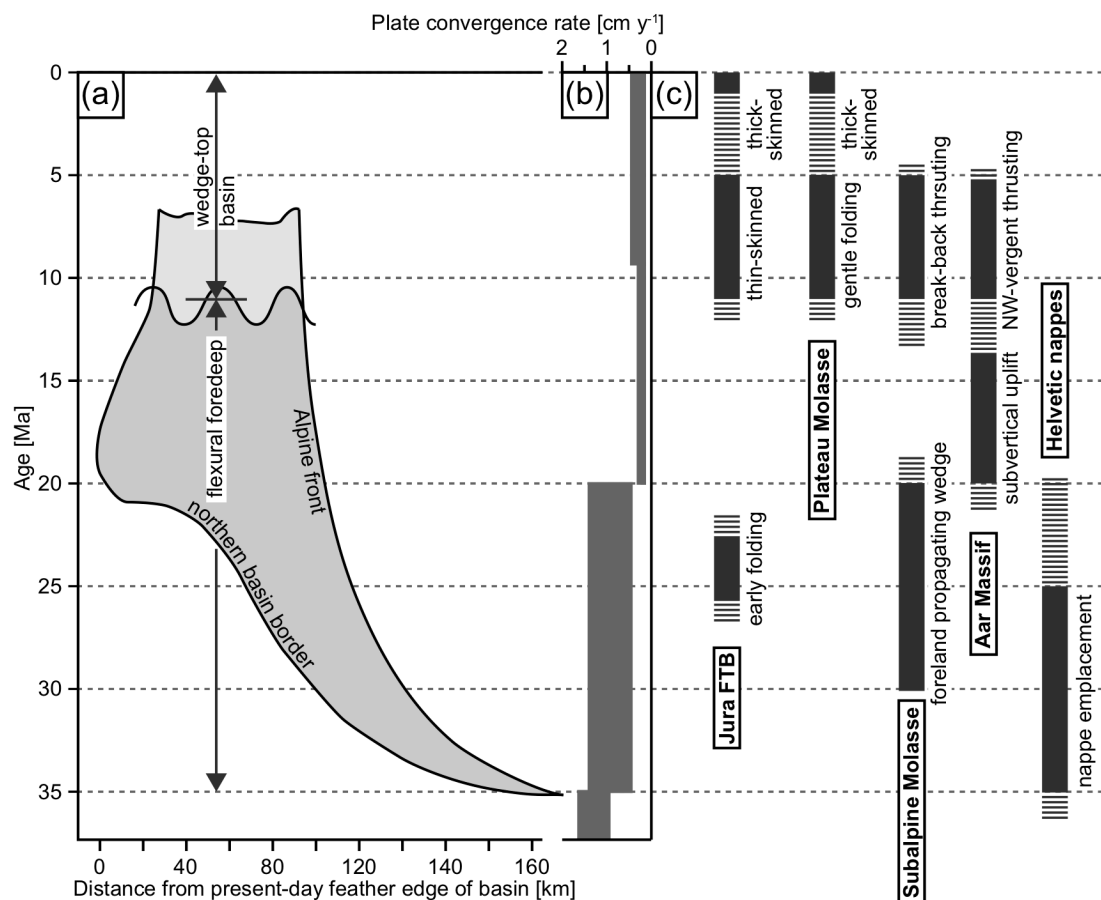
Fig. 8 Oligocene to present-day evolution of the northern Central Alps. (a) Temporal evolution of the Molasse Basin architecture (adapted from Schlunegger and Kissling, 2015). The location of the section is given in Fig. 1. (b) Rates of plate convergence between Adria and Europe (Handy et al., 2010; Schmid et al., 1996). (c) Tectonic evolution of the major tectonic units of the northern Central Alps. FTB, fold-and-thrust belt
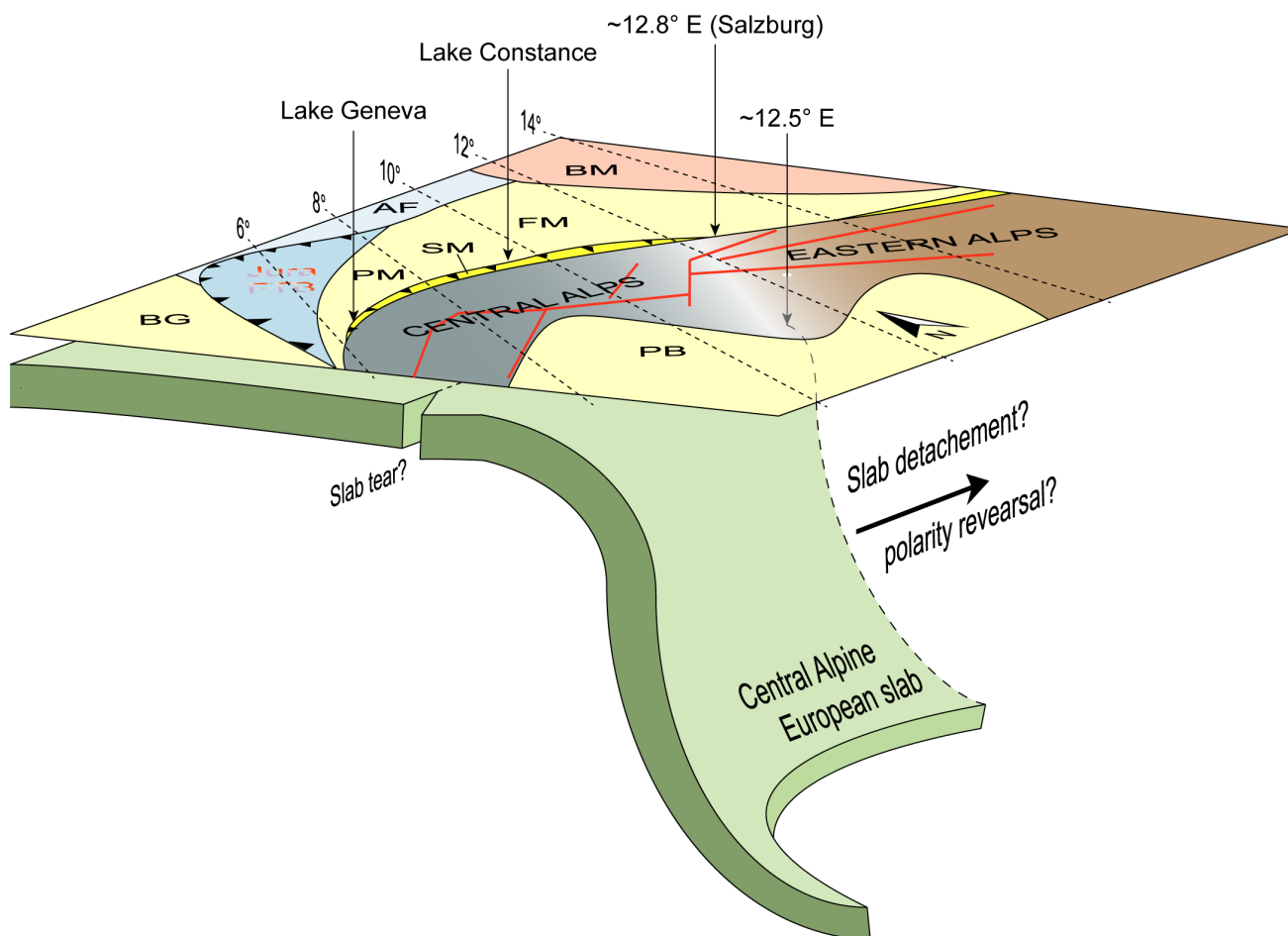
Fig. 9 Schematic 3D representation of the structure of the Central Alpine European slab and its spatial correlation with the eastward termination of the late Miocene Subalpine Molasse near Salzburg. PM, Plateau Molasse; FM, Foreland Molasse; SM, Subalpine Molasse; PB, Po Basin; TW, Tauern Window; BF, Brenner Fault; FTB, Fold-and-thrust belt; BG, Bresse Graben; AF, autochthonous foreland; BM, Bohemian Massif.